Applied Electronics Laboratory
Stanford University
Stanford, California

A HIGH-POWER S-BAND BACKWARD-WAVE OSCILLATOR

by

J. L. Putz
and
W. R. Luebke

Technical Report No. 182-1
February 24, 1956

Prepared under Signal Corps Contract DA36-039-SC-63189
and under Office of Naval Research Contract
N6onr 25132 (NR 373 362)
Jointly supported by the U. S. Army Signal Corps,
The U. S. Air Force, and the U. S. Navy
(Office of Naval Research,
Bureau of Ships, and Bureau of Aeronautics)

SUMMARY

The tubes described in this report are S-band backward-wave oscillators of the folded-line type with a nominal power output of 100 watts cw. These oscillators were developed under Stanford Electronics Research Laboratory Projects 182 and 185.

Both continuously pumped and sealed-off versions are described, but experimental results are given for only the demountable tubes. These tubes operated over the frequency range 2.5 - 3.5 kMC, with a power output of about 75 watts at the low-frequency end, and 100 - 150 watts at the high-frequency end. The efficiency varied between 6 and 12 per cent. The experimental results agree very well with theory.

Detailed design information for the folded-line type of BWO is presented in an Appendix, mostly in the form of charts.

TABLE OF CONTENTS

LIST OF ILLUSTRATIONS

LIST OF SYMBOLS

Symbol	Definition	Defining equation or figure
a	hole radius	Fig. A-1
b	velocity parameter	(A-16)
C	gain parameter	(A-6),(A-11)
C_1	first approximation to C	(A-21)
c	velocity of light = 3×10^8 meters/s	
D	structure dimension	
F_1	plasma frequency factor	(A-15)
F_2	function relating starting CN and space-charge parameter	Fig. A-6
h	structure dimension	Fig. A-1
I_o	d-c beam current (amperes)	
I_{start}	d-c beam current for start-oscillation (amperes)	
$I_n(x)$	modified Bessel function of the first kind, order n, argument x	
K	tube constant	(A-20)
ℓ	interaction gap length	Fig. A-1
L	structure period	Fig. A-1
M	impedance reduction factor	(A-7)
N_{start}	number of start-oscillation beam wavelengths	(A-17)
P	total r-f power transmitted on the circuit	
Q'	space-charge parameter	(A-19)
r	beam radius	
R_1	component of impedance reduction factor due to variation of field across the beam	(A-8)

LIST OF SYMBOLS (Cont'd)

Symbol	Definition	Defining equation or figure
R_ω	plasma frequency reduction factor	
u_o	d-c beam velocity	
V	peak r-f voltage across the gaps	
V_o	d-c beam voltage	
V_{-1}	"circuit" voltage corresponding to v_{-1}	(A-2)
v_{-1}	phase velocity of the first "backward" mode on the circuit	(A-1)
W	structure dimension	Fig. A-1
Z_o	characteristic impedance of the line (ohms)	(A-5)
α	v_{-1}/u_o	
β	phase constant of the circuit	(A-1)
β_e	phase constant of the beam	(A-10)
γ	radial propagation constant	(A-9)
η	efficiency	Fig. A-6
η_o	"unadjusted" efficiency	Fig. A-6
λ_o	free-space wavelength	
ρ	dummy variable	
ω	operating frequency (radians/sec)	
ω_q	reduced plasma frequency (radians/sec)	(A-13)

PART 1.--TUBE TYPE S-182

I. INTRODUCTION

The tubes described in this part of the report are S-band backward-wave oscillators of the folded-line type with a nominal power output of 100 watts cw. These oscillators were developed under Stanford Electronics Research Laboratory Project 182, and are designated generally as S-182, with additional letters and numerals indicating various modifications.

S-182 is a continuously pumped, demountable tube designed to permit easy modification of the structure and gun. Several versions of this tube were tried, two of which are described in this report.

II. S-182 SPECIFICATIONS

The basic structure of tube type S-182 is a folded-strip transmission line with an axial hole for the beam. Figure 1 shows the form of the structure and the notation used for dimensions.

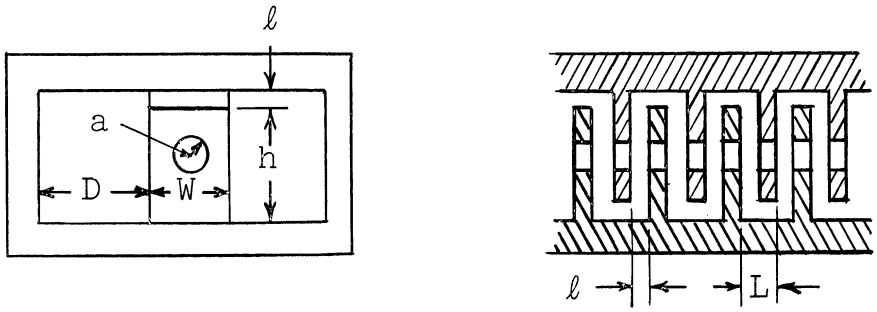

FIG. 1.--Folded-line structure.

The requirements for this tube were (1) a power output of 100 watts cw, (2) a tuning range from 2500 to 3500 MC, and (3) a beam voltage of about 3000 volts at the center frequency.

Using the design procedure given in Appendix A, the following dimensions for the tube structure were arrived at:

L = 0.140 in.
ℓ = 0.080 in.
h = 0.600 in.
W = 0.400 in.
D = 0.600 in.
a = 0.063 in.
Length = $6\frac{1}{2}$ in. (active)
Cathode diameter = .090 in.

This version of the tube is designated S-182-A. Figure 2 is a photograph of the tube, and Fig. 3 is a cross-sectional view showing some of the mechanical details. All parts of the tube body are made from OFHC copper except the r-f line bead seals, which consist of Teflon, and the collector seal which utilizes ceramic. The gun is mounted inside the vacuum manifold, giving a large pump-out cross-section. All joints are soft-soldered, or sealed with wax. Water-cooling is provided for the collector and on the tube body to protect the wax seals.

A later version of this tube, designated S-182-H2, is identical with S-182-A except for the beam hole size, the tube length, and some minor modifications of the collector and the r-f matches. For S-182-H2:

a = 0.0938 in.
Length = 5.5 in. (active)
Cathode diameter = .150 in.
All other dimensions are the same as those given for type S-182-A

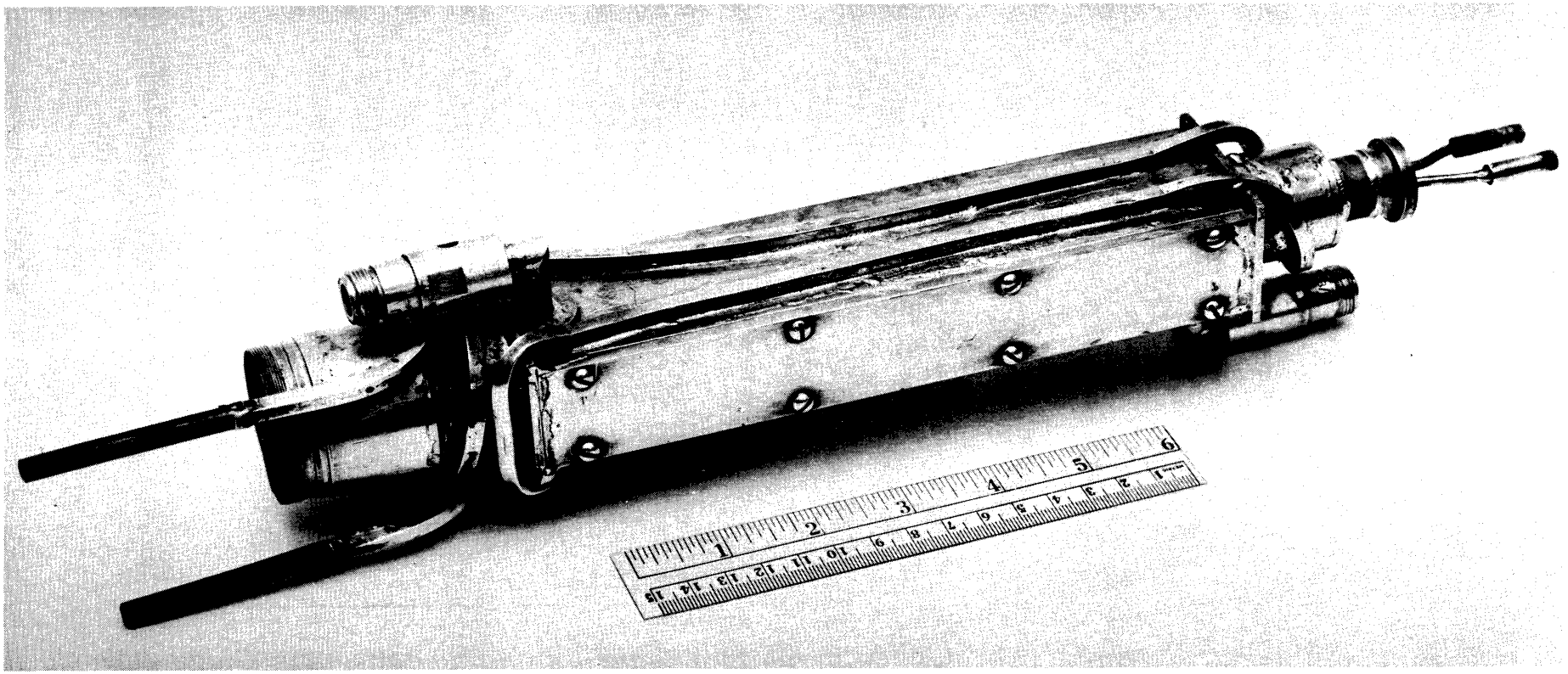

FIG. 2.--100-watt S-band tube type S-182-A.

III. S-182 OPERATING CHARACTERISTICS

A. MATCHES AND INSERTION LOSS

The problem of matching from a 50-ohm coaxial line to the folded-line structure was solved by attaching the center conductor of the coaxial line to one of the "teeth" of the interdigital structure and providing a short-circuit a quarter of a wavelength beyond the junction. (See Fig. 3.) This type of match is very similar to that used for ridge-guide to coaxial lines. In addition, the center conductor of the coaxial line was tapered over a length of about two inches in an attempt to provide a gradual transition from the 50-ohm impedance of the coaxial line to the somewhat higher impedance of the structure.

For satisfactory operation, the r-f match at the collector end of the tube should be as good as possible. If reflected energy from the load is re-reflected at the collector end, the resulting degenerative or regenerative feed-back will cause the output to vary rapidly with frequency. In order to improve the match at the collector end, some internal loss was added in the form of a carbon film on ceramic plates, placed next to the folded line for approximately the last two inches. The ceramic plates were cut at an angle to produce a gradual transition to the lossy region. The position of these "pads" can be seen in Fig. 3. Two plates were used in tube S-182-A, one on each side of the line. The surface resistivity of the carbon film was about 300 ohms per square. In tube S-182-H2, only one plate was used, with a resistivity of about 500 ohms per square.

Figures 4, 5, and 6 show the measured matches and insertion loss for both S-182-A and S-182-H2. Without the "pads", the insertion loss was less than 1 db.

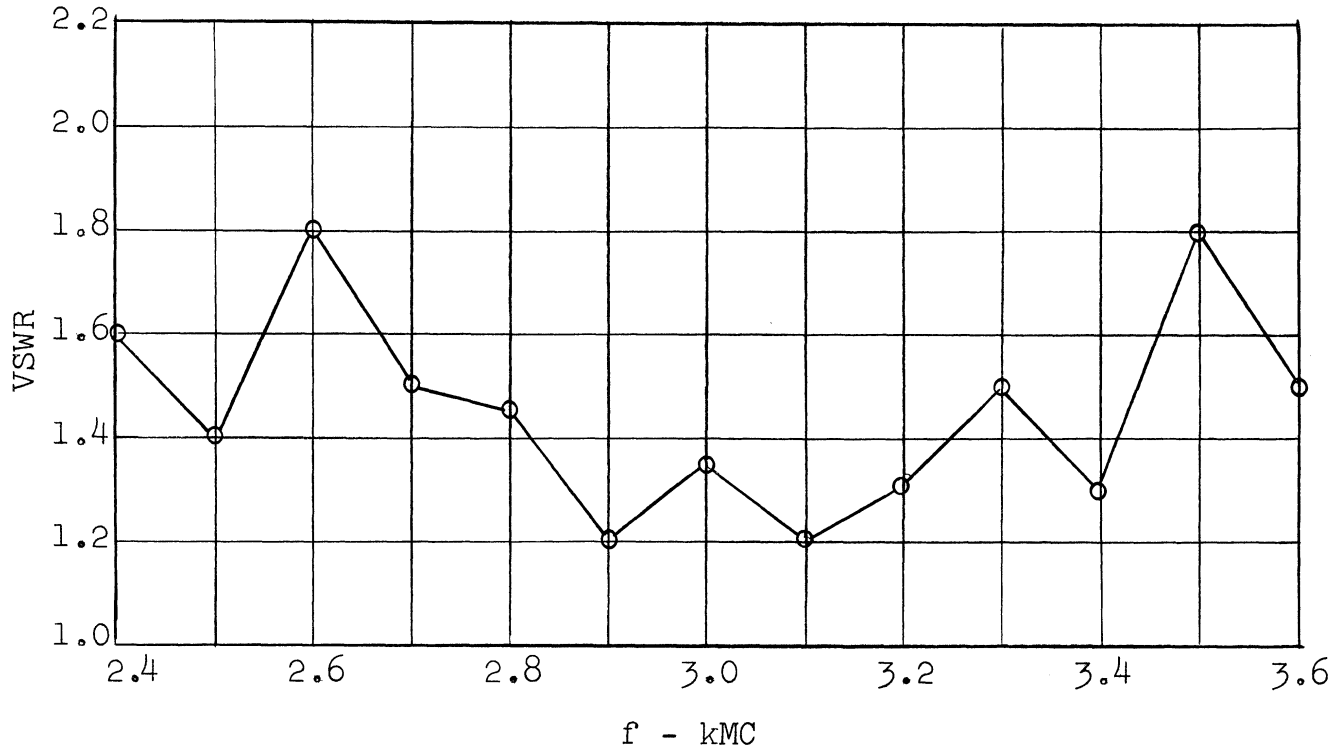

FIG. 4.--Gun-end VSWR of S-182-A with the collector end terminated in a 50-ohm load.

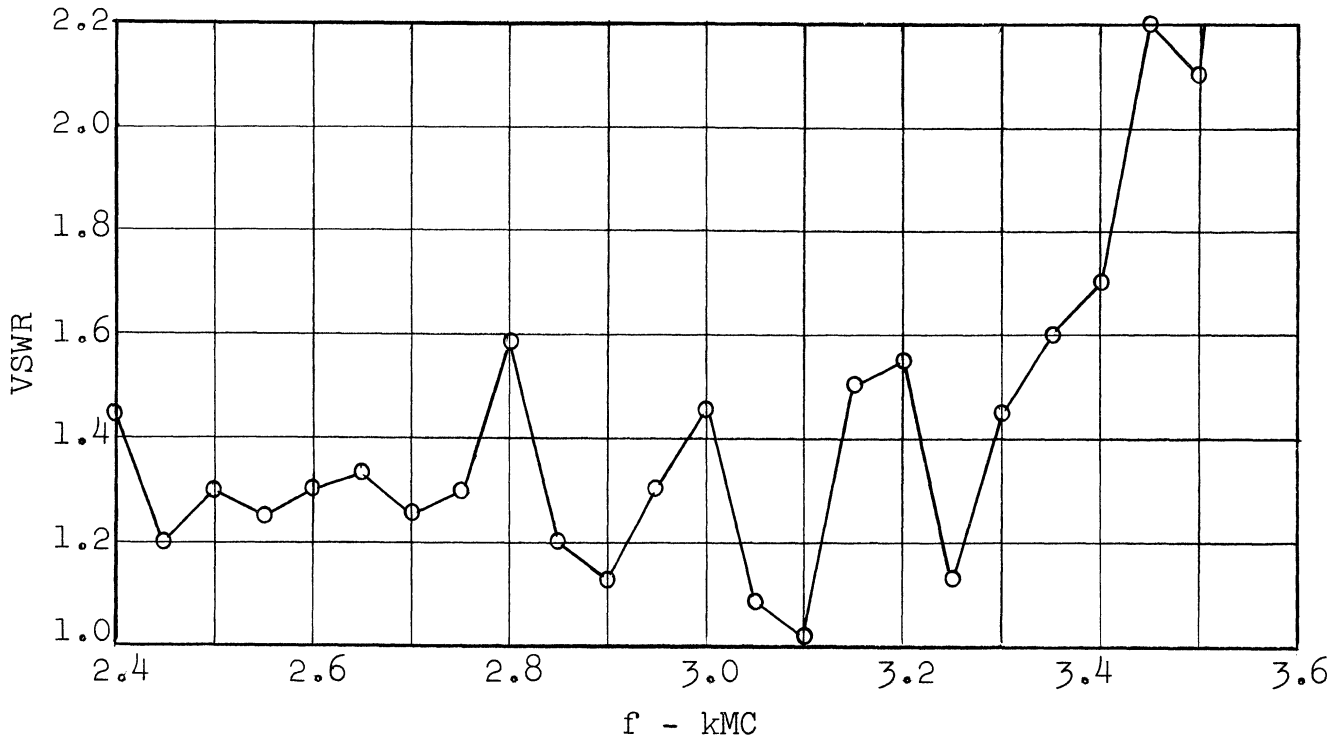

FIG. 5.--Gun-end VSWR of S-182-H2 with the collector end terminated in a 50-ohm load.

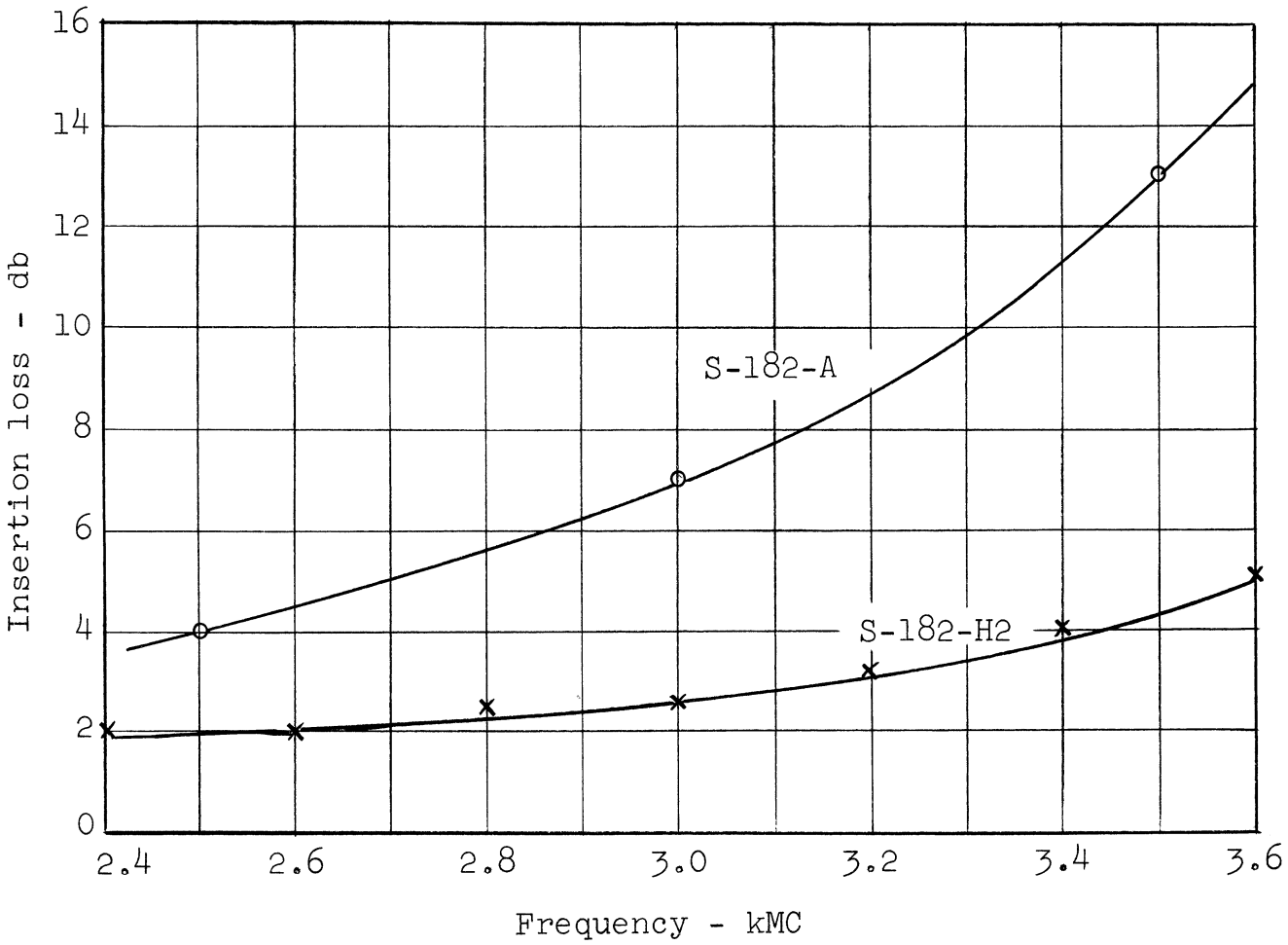

FIG. 6.--Insertion loss of S-182-A and S-182-H2 with internal "pads" in place.

B. TUNING CURVES

Figure 7 shows the tuning curves for tube S-182-A. The effect of beam current on frequency ("frequency pushing") is readily apparent. A comparison of the calculated and extrapolated zero-current curves shows that the simple picture of a wave following around the folded-line structure is somewhat in error.

A better comparison between the theoretical and actual (extrapolated) propagation velocity is given by Fig. 8. For

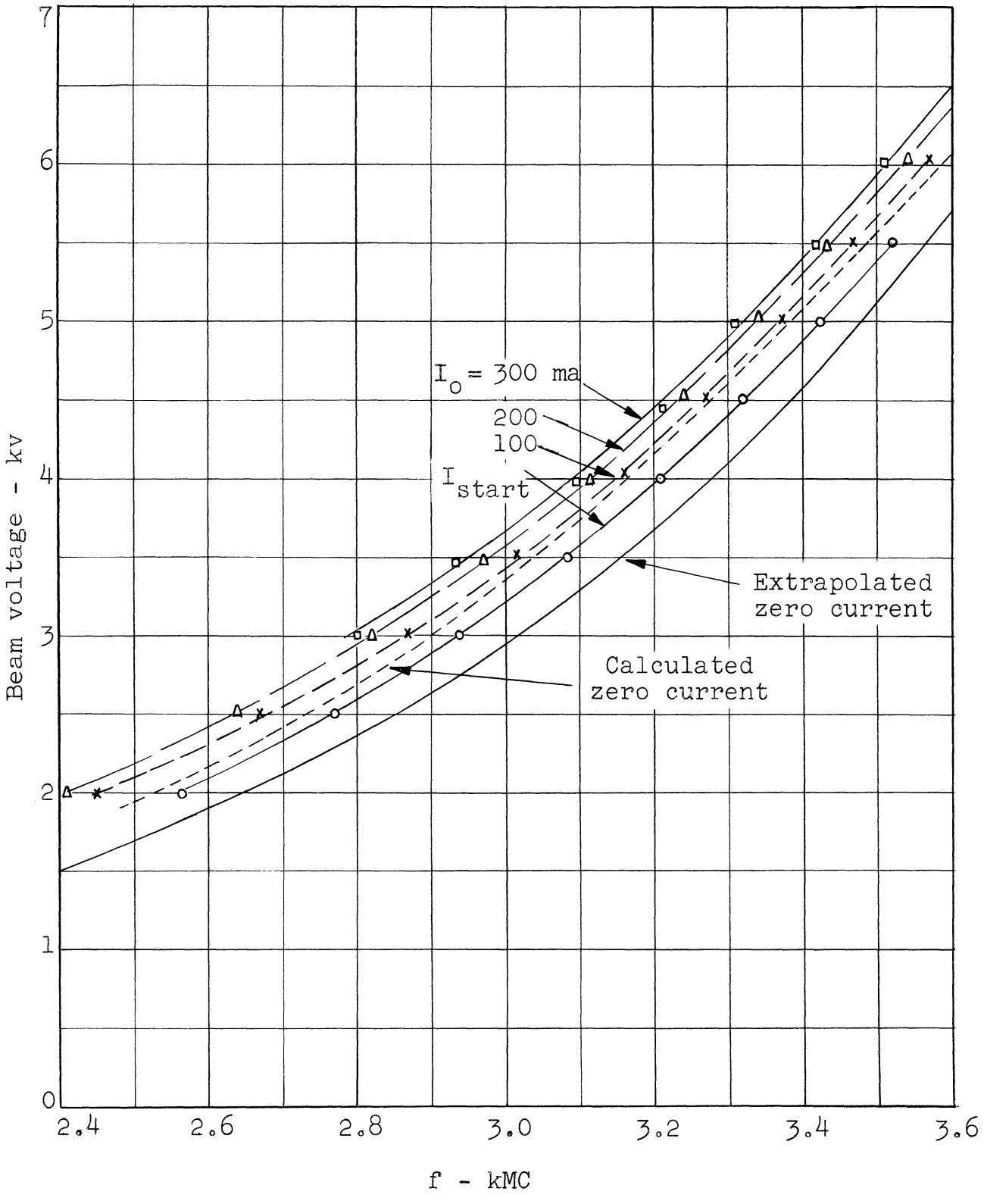

FIG. 7.--Tuning curves for tube S-182-A. Note the large "frequency pushing" effect.

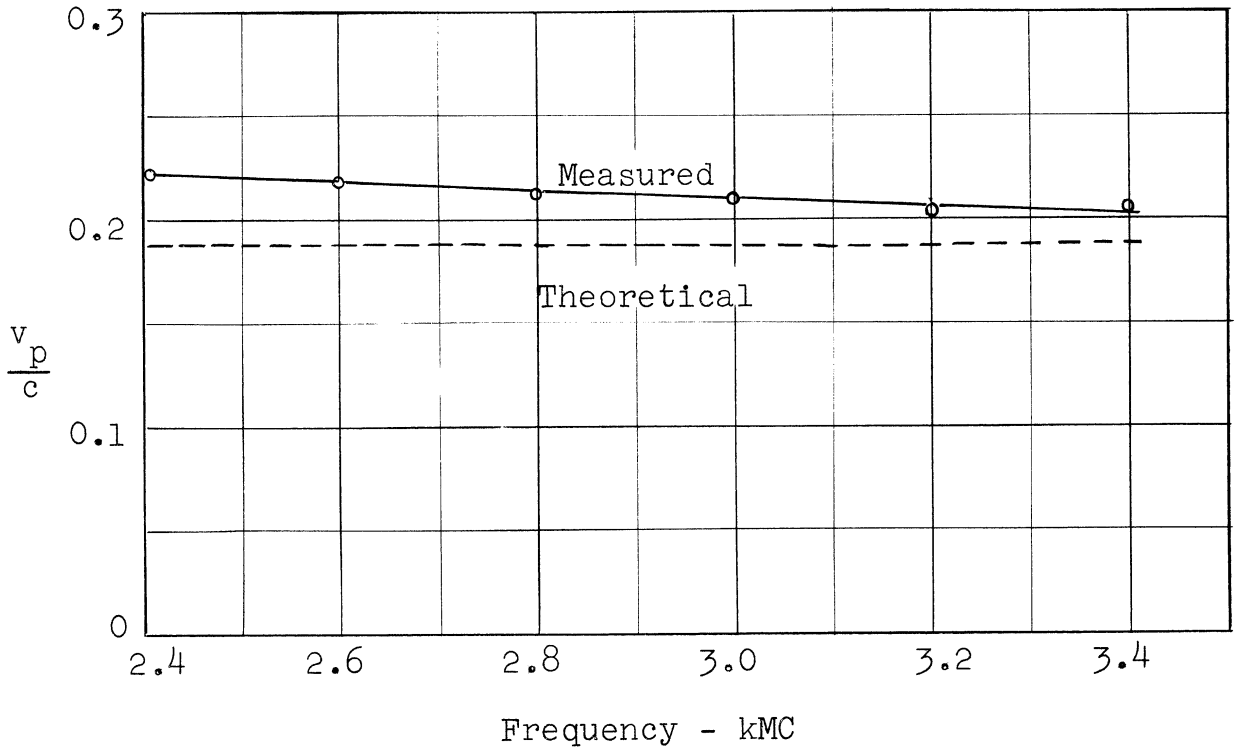

FIG. 8.--Comparison of measured and theoretical phase velocities for the folded-line structure of S-182.

this figure, the "fundamental" phase velocity of the wave is defined by:

$$\frac{v_p}{c} = \frac{\text{Period length}}{\text{Free-space wavelength}} \cdot \frac{2\pi}{\theta} \qquad (1)$$

where c is the velocity of light, and θ is the phase shift per period neglecting the 180°-shift introduced by the fold in the line. If the wave followed the folded line exactly, the "geometric" ratio of the phase velocity to the velocity of light would be $v_p/c = L/(L + h)$. Figure 8 indicates that the actual phase velocity is greater than the "geometric" value by about 5 to 15 per cent.

The tuning curves for tube S-182-H2 were essentially the same as those for S-182-A, except for a narrow "hole" at

2975 MC. This discontinuity was traced to a resonance in the pumping manifold. The enlarged beam hole was apparently responsible for the coupling between the manifold and the structure. Presumably, such a coupled resonance could be eliminated by proper design.

C. POWER OUTPUT AND EFFICIENCY

The power output and efficiency of tubes S-182-A and S-182-H2 are shown in Figs. 9 to 12, inclusive. The theoretical efficiency curves shown are based on the theory developed by R. W. Grow.[1] The results of this theory which apply to the folded-line type of tube are presented in Appendix A. The agreement between the theoretical and measured efficiencies is very good, considering the fact that the effective size of the beam is not accurately known.

Figure 13 shows an oscilloscope tracing of the power output of S-182-H2 as indicated by a crystal detector, while sweeping the beam voltage at 60 cps over the entire tuning range. The response of the crystal detector was flat within ± 0.5 db over the frequency range of interest. The rapid changes of power output with frequency near the high-voltage end of the range can be correlated with mismatches in the tube. (See Fig. 5.) In other respects, the power output appears to be fairly smooth. The beam current is not exactly constant for the curves shown since the current depends to a small extent on the voltage, but the total current variation from one end of the range to the other is less than 10 per cent.

As seen from the curves, the efficiency of S-182-A is higher than that of S-182-H2. This higher efficiency is the result of the greater beam current density used in S-182-A ($7 a/cm^2$, as compared to $2.5 a/cm^2$ used in S-182-H2). In order

---

[1] Superscript numerals refer to the List of References that appears at the end of the report.

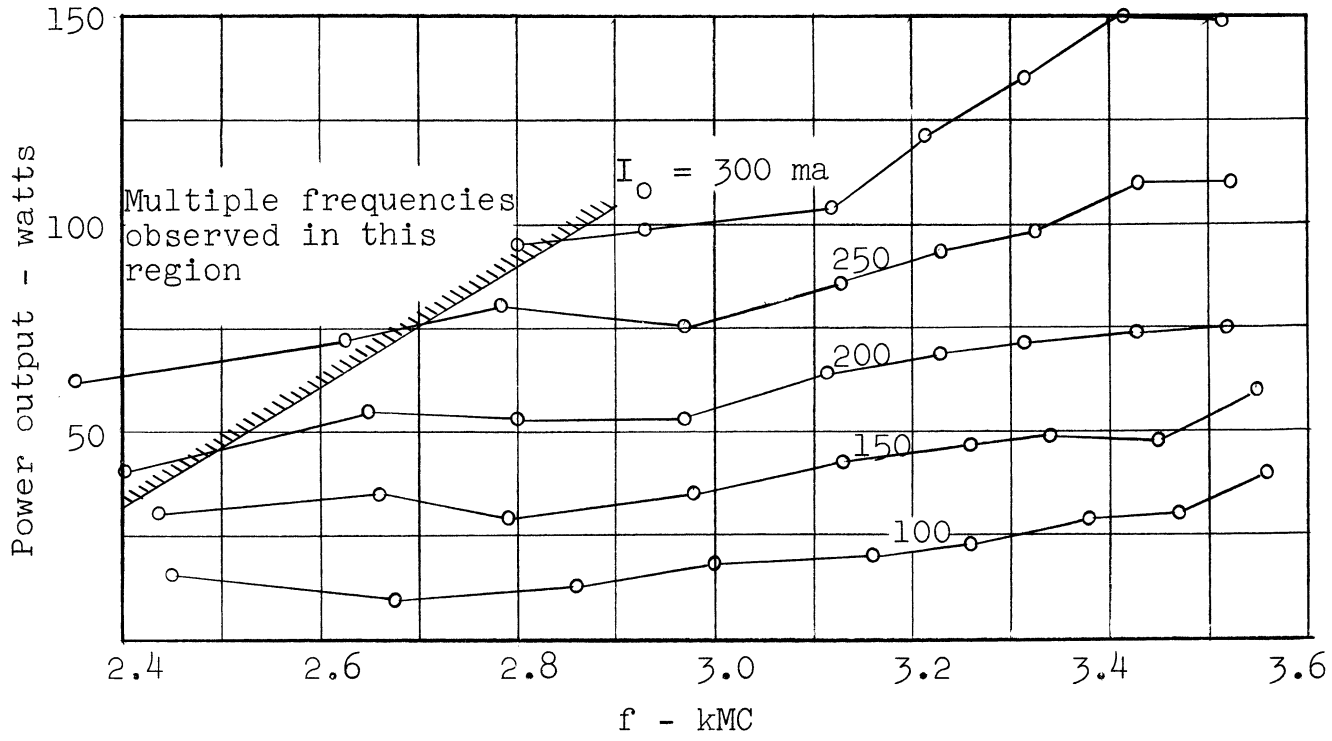

FIG. 9.--Power output of S-182-A for various beam currents. An axial magnetic field of 1800 gauss was needed for high beam currents.

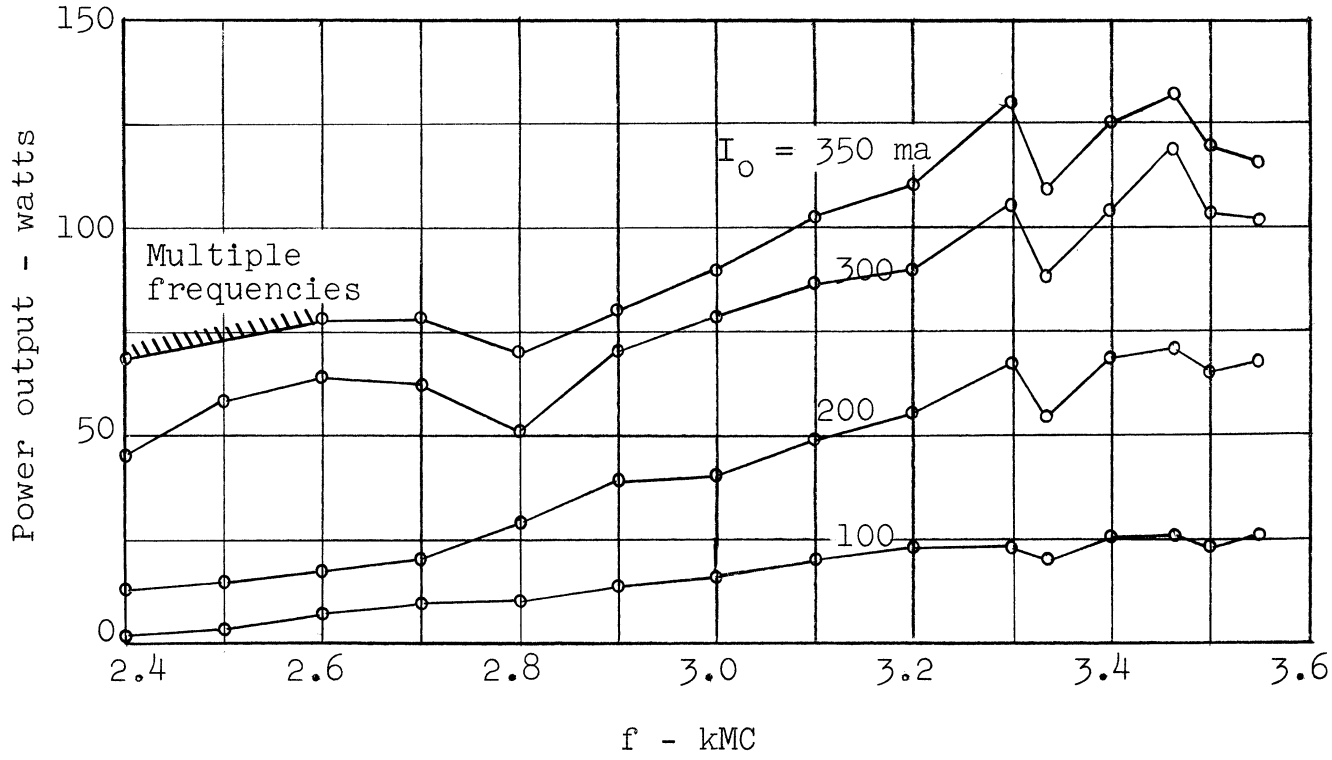

FIG. 10.--Power output of S-182-H2 for various beam currents. Focus field = 1250 gauss.

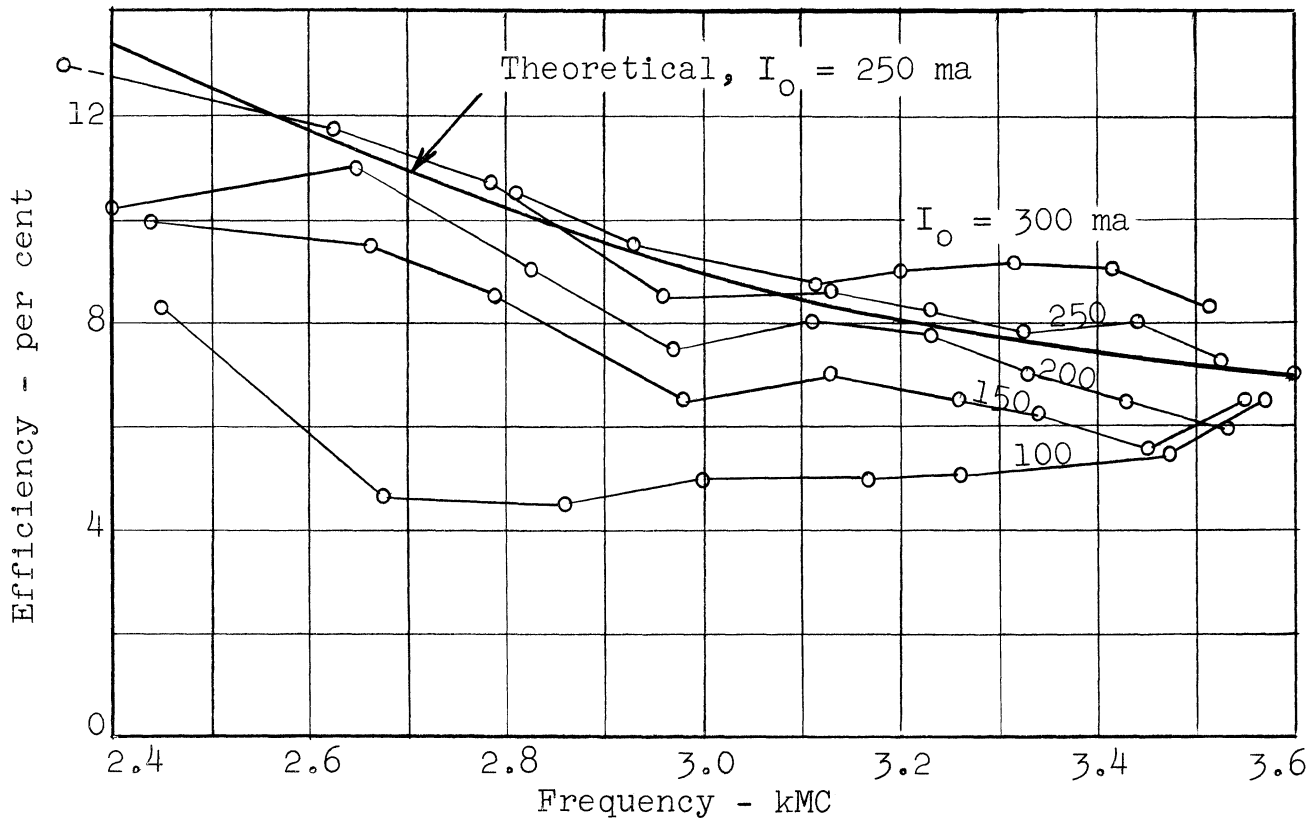

FIG. 11.--Efficiency of tube S-182-A.

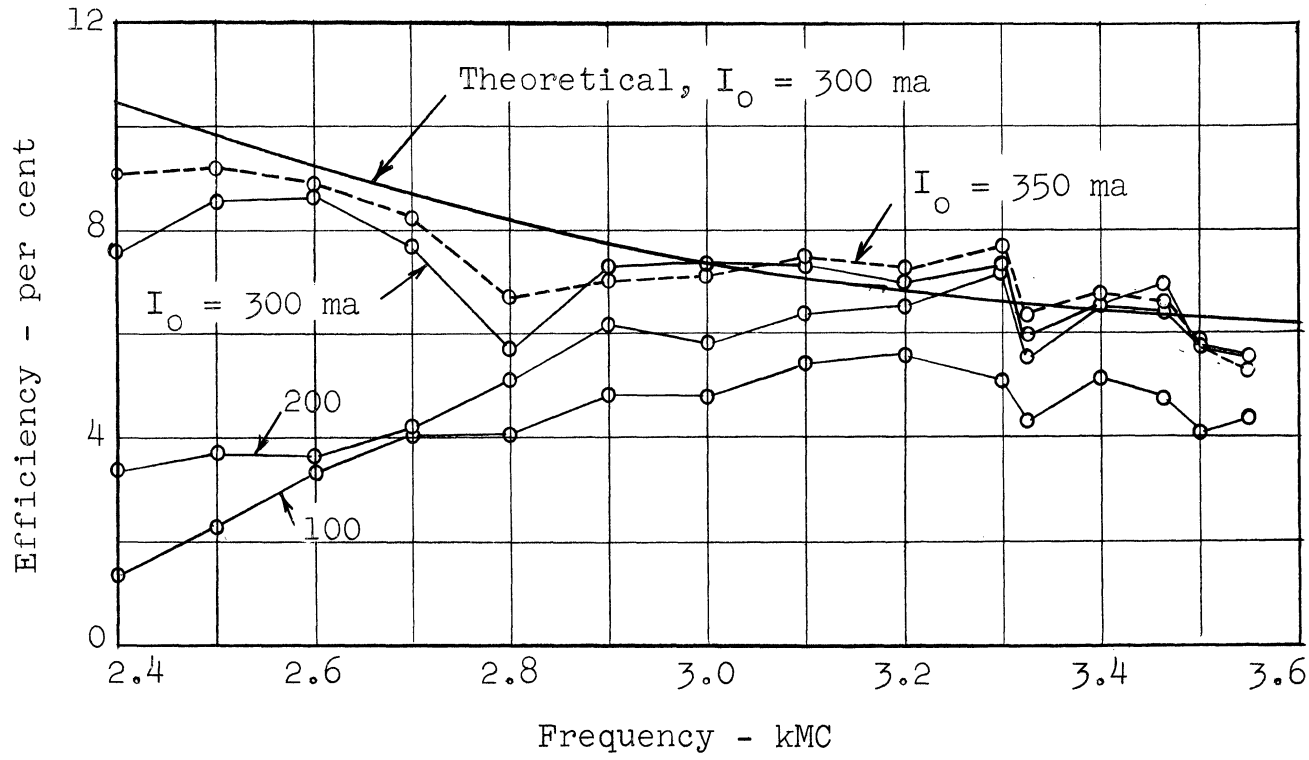

FIG. 12.--Efficiency of tube S-182-H2.

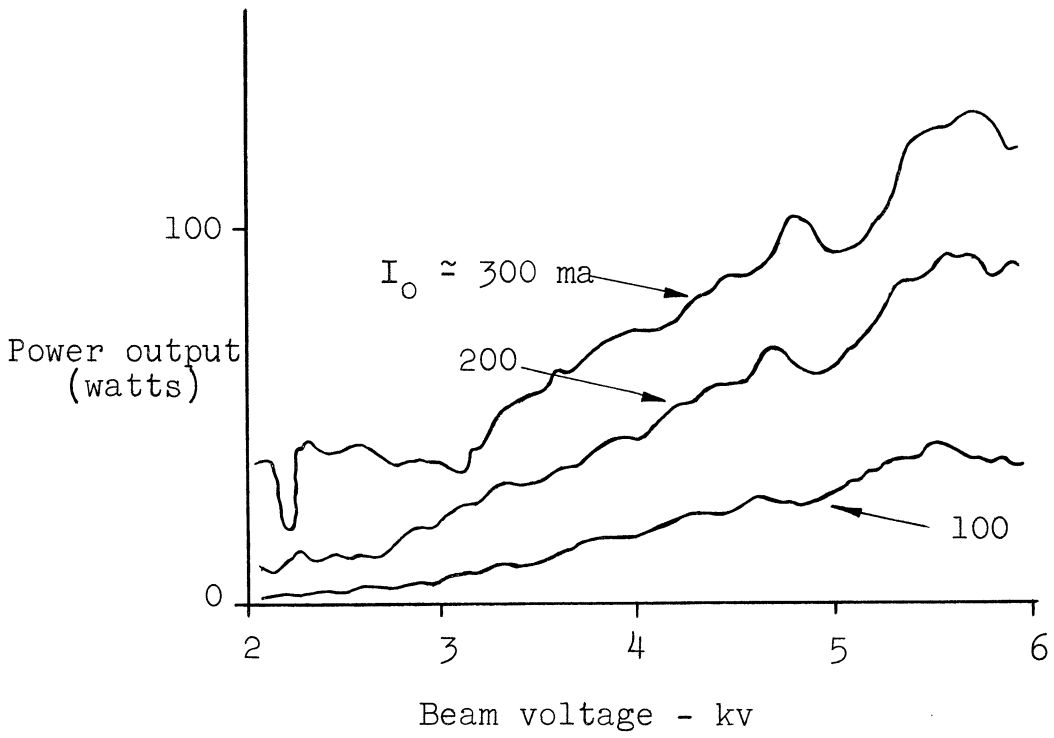

FIG. 13.--Oscilloscope tracing of the power output of tube S-182-H2 as a function of beam voltage, for several beam currents. Compare with Fig. 10.

to obtain good tube life at the higher current density, a convergent-flow gun might have to be used; this is one possible disadvantage of this type of operation. (In the experimental tubes, life was not important, so confined-flow guns were used.)

D. STARTING CURRENTS

Figures 14 and 15 show the start-oscillation current as a function of frequency for S-182-A and S-182-H2, respectively. Again, the agreement with theory is fairly good, considering that the active lengths of the tubes are not accurately known owing to the presence of the internal attenuators.

E. SPURIOUS OUTPUTS

As shown by Fig. 9, multiple frequencies were observed at the low-frequency end of the tuning range in tube S-182-A. Under the worst conditions, as many as ten extra frequencies were observed in the output. These frequencies were spaced at about 50 MC-intervals on either side of the normal operating frequency. The strengths of these extra outputs increased rapidly with increasing beam current, the strongest reaching an output level perhaps 5 - 10 db below the main output, in some cases.

One explanation for these multiple outputs is that higher-order solutions of the equations describing the start-oscillation conditions are possible if the value of CN is large enough. (See Reference 2.) These solutions indicate that, for a given beam voltage, the frequency of a higher-order oscillation would be slightly lower than the normal operating frequency. Since a backward-wave oscillator is not "saturated" in the usual sense, it also appears possible that the tube could oscillate on two frequencies at the same time. The presence of more than two frequencies in the output has been explained by Johnson[3] as being the result of intermodulation effects in the beam.

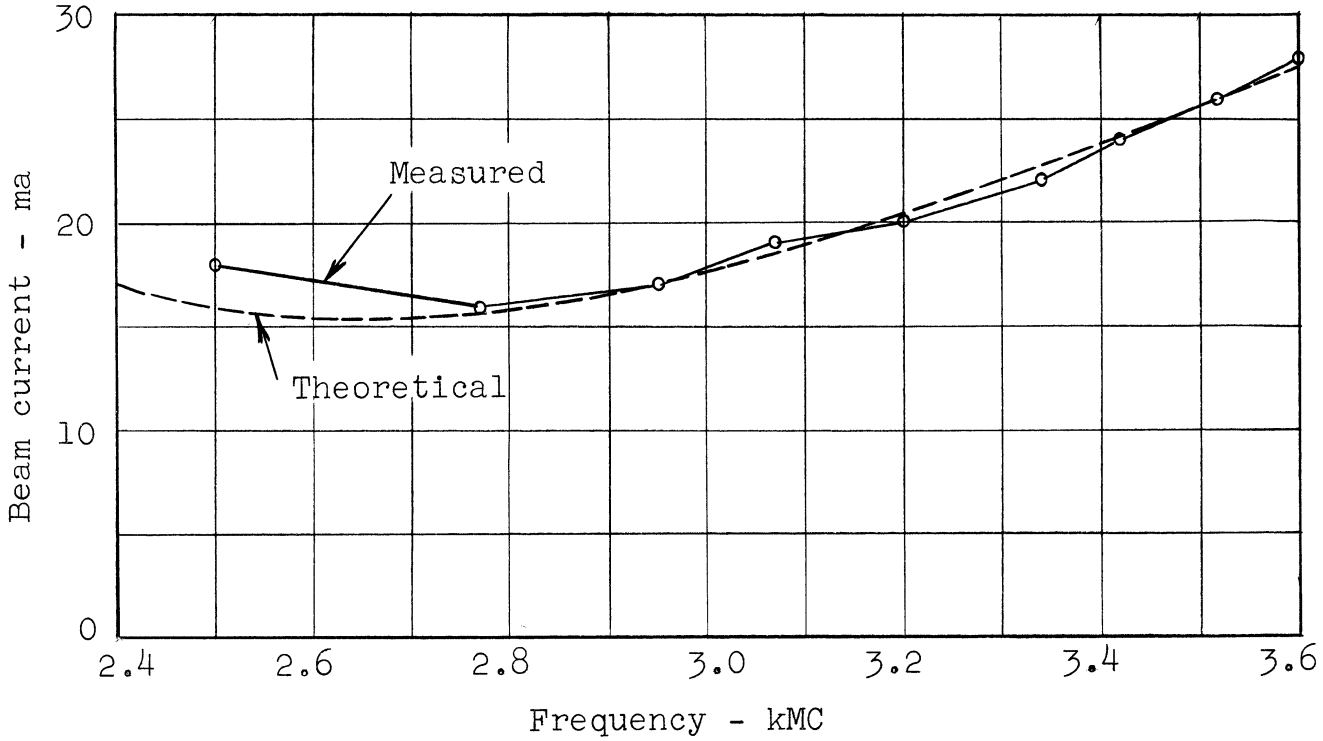

FIG. 14.--Starting current for tube S-182-A.

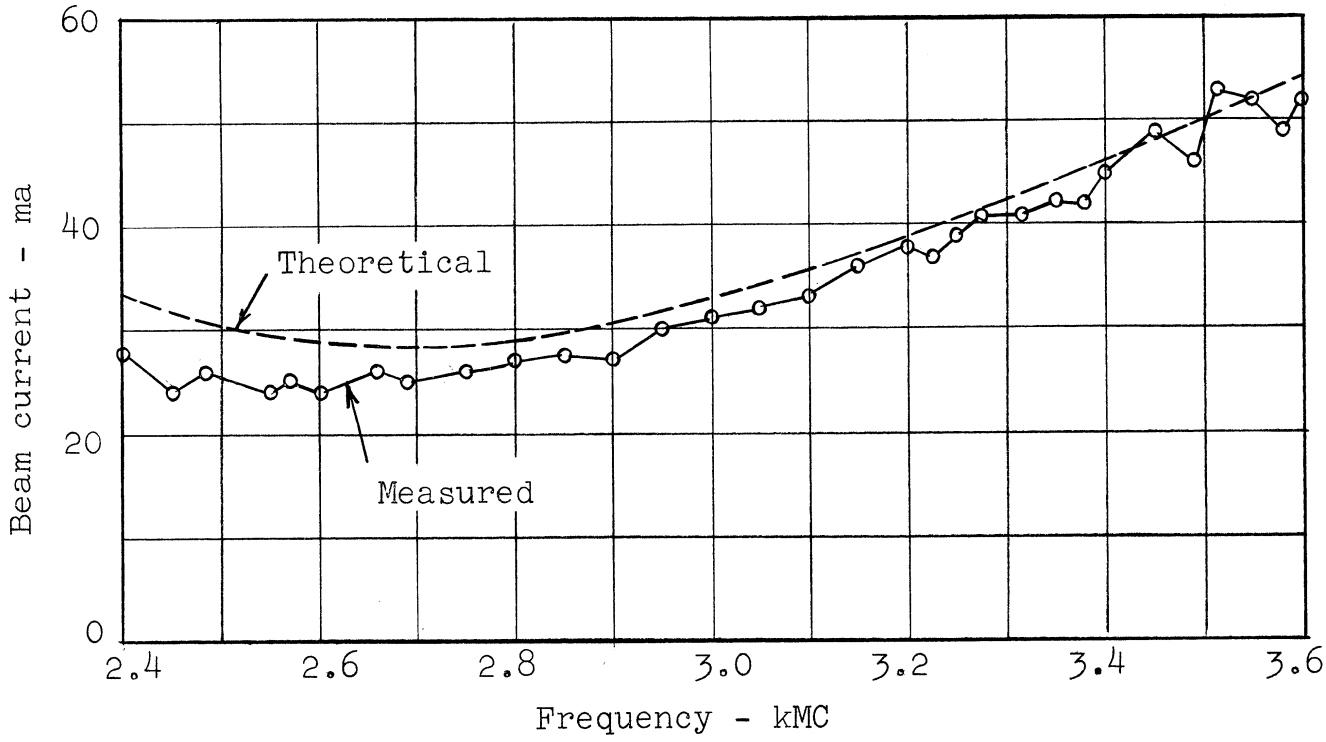

FIG. 15.--Starting current for tube S-182-H2.

As was expected, multiple frequencies did not appear in tube S-182-H2, except at the very highest perveances. The shorter length (5-1/2 in. as compared to 6-1/2 in. for S-182-A) made the starting current for the spurious oscillations higher than the normal operating current of 300 ma.

IV. CONCLUSIONS

It appears that the performance of the folded-line type of BWO can be satisfactorily predicted from the usual theory of BWO operation, both as to tuning range and efficiency. In addition, the essentially all-metal construction of this type of tube provides good heat transfer away from the interaction circuit, thus minimizing the problem of heat dissipation in a high-power tube. The circuit is relatively large, and scaling according to wavelength should be possible, with the power output varying as λ^4 for constant beam current density.

PART 2.--TUBE TYPE S-185

I. INTRODUCTION

This part of the report will be chiefly concerned with a description of some of the techniques used in the construction of tube S-185, the designation given to the sealed-off version of the S-182 demountable tube described previously. A photograph of the tube is shown in Fig. 17, and Fig. 16 is an assembly drawing which shows most of the mechanical details of the tube.

The general specifications of tube S-182 were used except that the length of the interaction structure was shortened to approximately 6 inches to eliminate some spurious frequencies at the low end of the tuning range. The hole for the beam was 0.120 in. Mechanical design changes were limited to those made necessary by the more rigorous processing schedule of sealed-off tubes. In general, these changes involved the substitution of high-temperature brazing alloys for soft solder, and the use of glass instead of Teflon for insulated vacuum seals.

II. SUB-ASSEMBLIES

A. BLOCKS AND END BELLS

The construction of the blocks was straightforward except for the problem of producing the long, straight hole for the beam. In the demountable tube, as in similar tubes previously built here, the hole was made by first milling semi-circular grooves in two blocks of OFHC copper. The blocks were then silver-plated, clamped together around an oxidized stainless steel mandrel and brazed together in a hydrogen furnace. After removing the mandrel, the r-f structure could be milled out.

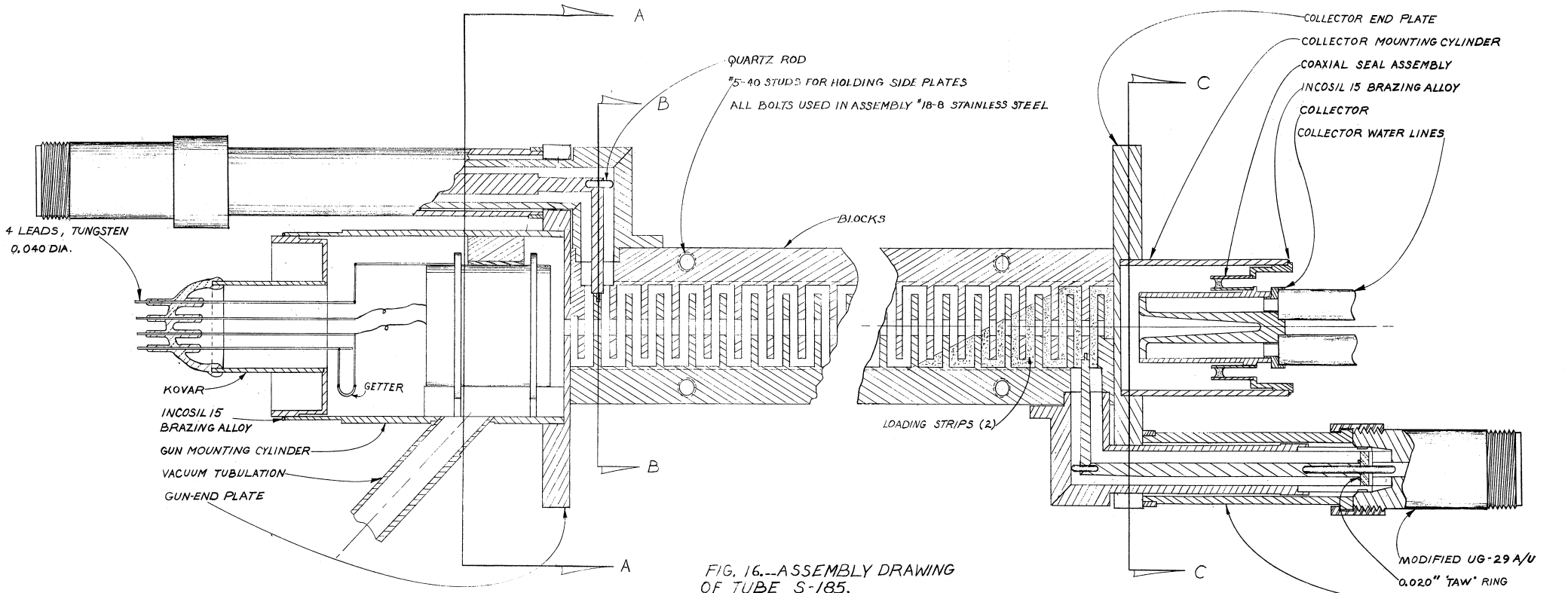

FIG. 16.--ASSEMBLY DRAWING OF TUBE S-185.

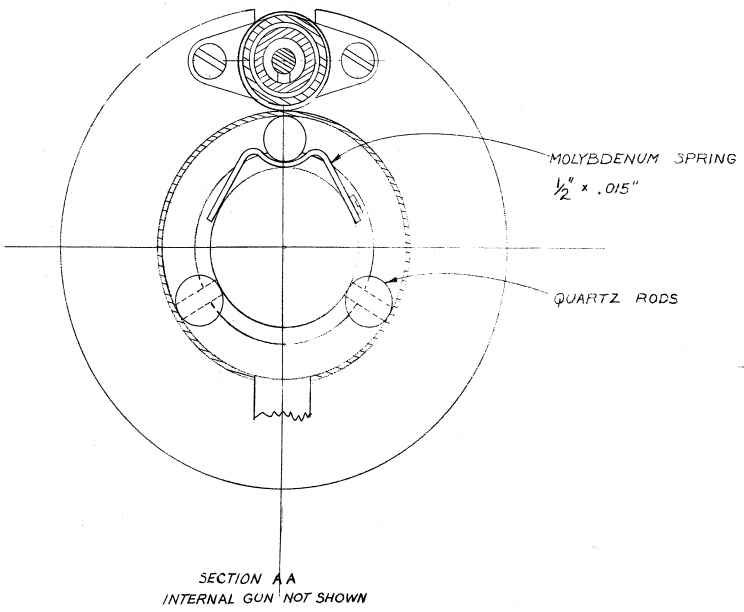

SECTION A A
INTERNAL GUN NOT SHOWN

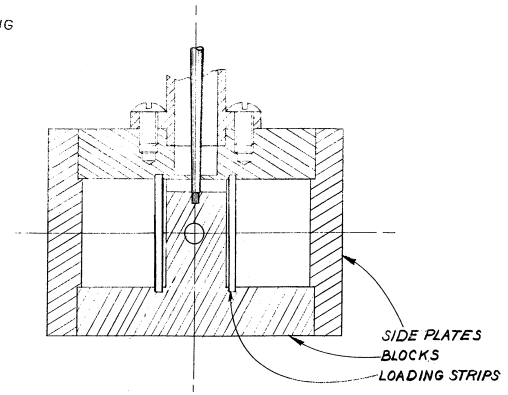

SECTION B-B

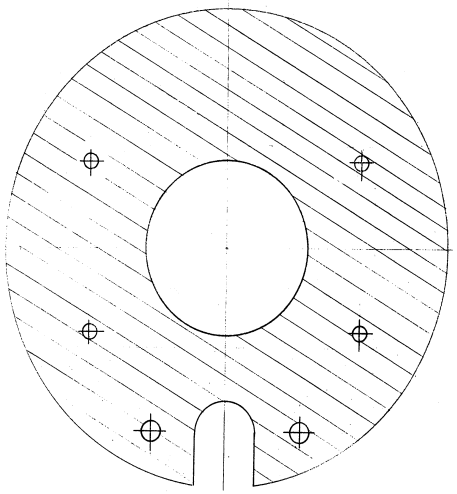

SECTION C-C
ATTACH HOLES SHOWN

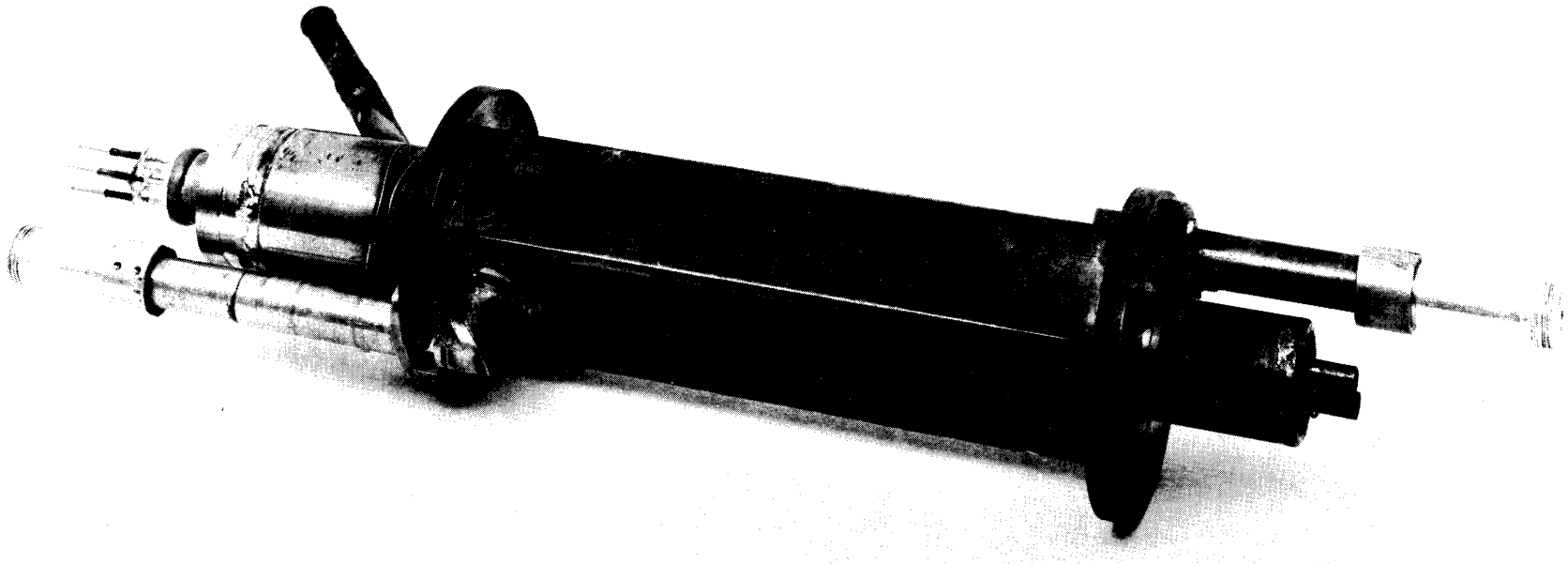

FIG. 17.--100-watt S-band tube type S-185.

The blocks for this tube were made in essentially the same manner, except that gold-plating was used, chiefly because it was thus possible to assemble the rest of the tube by using the silver-plating technique. In addition, since the mandrels had always been difficult to remove, only two short sections of ceramic rod were used at the ends of the blocks to align the section during the brazing operation. These end plugs were cut off during subsequent machining operations.

The plating thickness of the gold was 0.0005 in., and the furnace temperature was raised until the brazing material flowed at about 950°C.

It was convenient to preassemble the end bells for the tube. These subassemblies, shown in Figs. 18 and 19, consisted of an end plate and a mounting cylinder for the collector end of the tube, and an end plate, mounting cylinder, and the vacuum tubulation, for the gun end of the tube. The brazing of these parts was carried out in a straightforward manner in a hydrogen atmosphere using copper-gold alloy (Cu-62.5, Au-37.5).

B. R-F LINES AND SEALS

The vacuum seals for the r-f lines were designed so as to introduce as little discontinuity as possible when placed in a standard 3/8-in. coaxial line using standard type-N fittings. The glass dielectric was made as thin as possible (less than 0.1 wavelength), and the size of the center conductor was chosen to produce a constant-impedance line.

Since the power level to be transmitted at the gun end of the tube was relatively high (approaching 100 w), it was necessary to have a bead assembly with very low loss. Such beads were constructed following a procedure described by Turnbull.[9] The Kovar parts were first copper-plated to produce high conductivity, and then given a flash coating of chromium which was oxidized, leaving a surface suitable for the glass-sealing operation. The steps in the process are enumerated in Fig. 20.

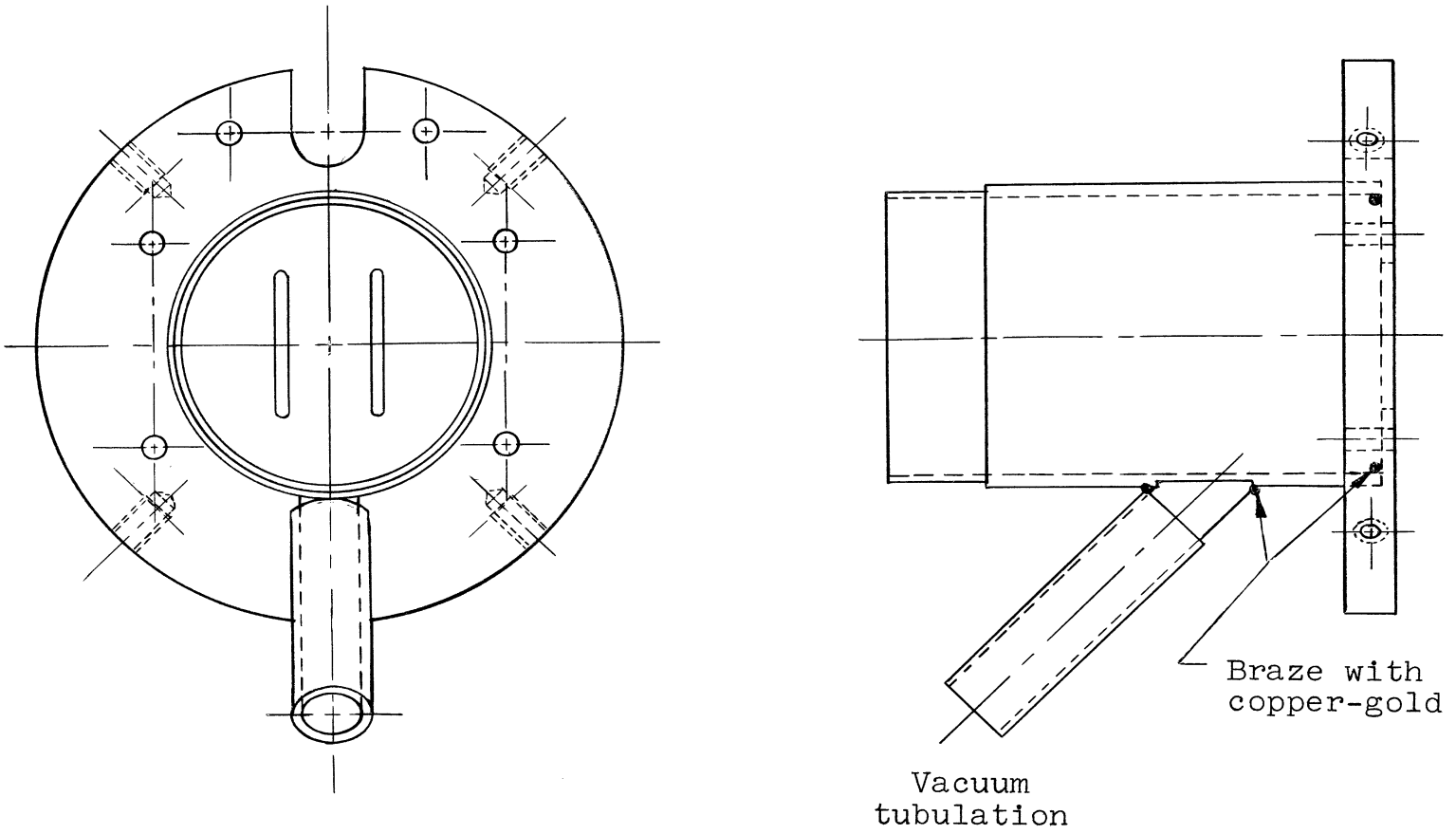

FIG. 18.--Gun end bell.

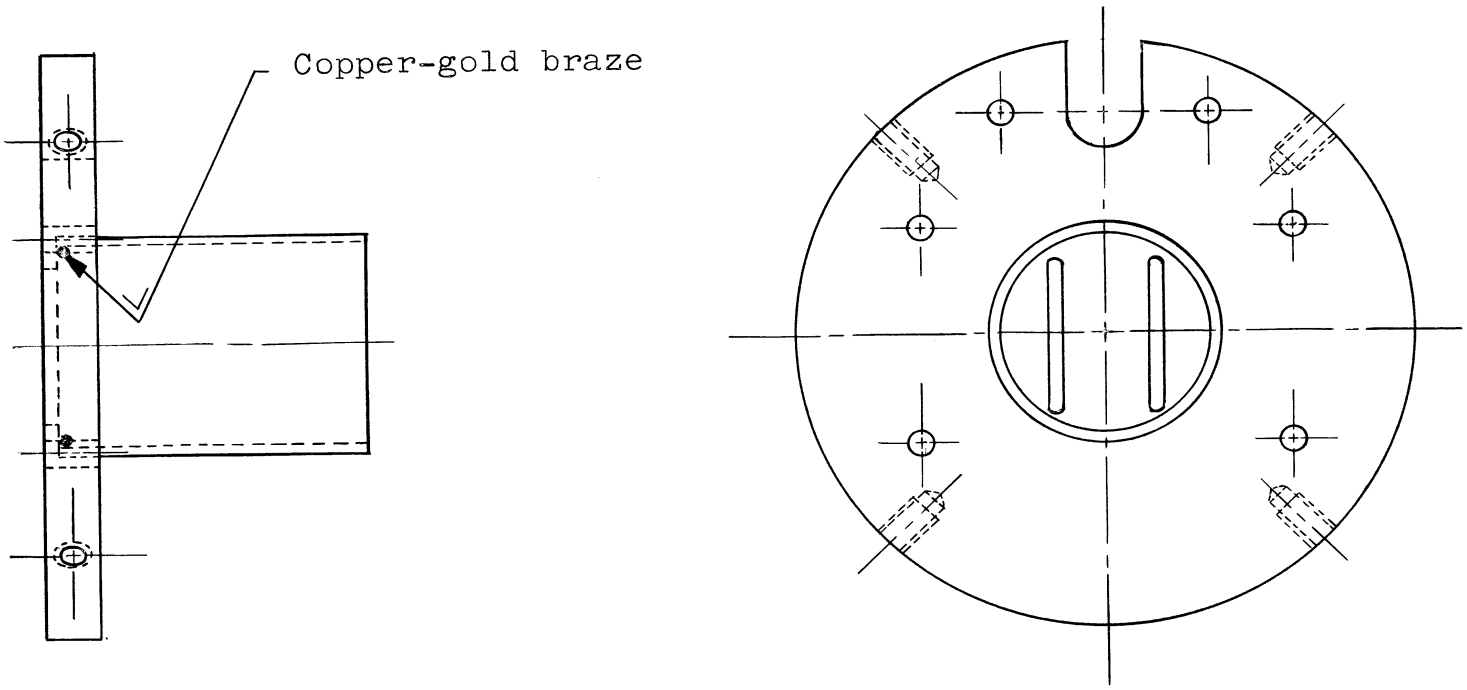

FIG. 19.--Collector end bell.

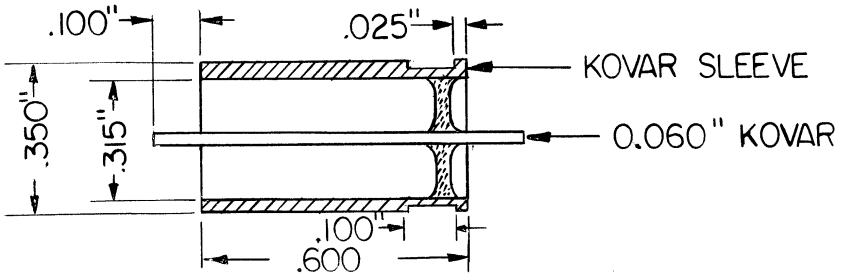

1. Polish rod and inside of sleeve.

2. Clean and degrease.

3. Fire in wet H_2 at 1000°C for 20 minutes.

4. Copper-plate all surfaces, 0.001 in. thick.

5. Fire in H_2 to check plating at 900°C for 15 minutes.

6. Chromium-plate only areas to be glassed, 0.00005-0.0001 in. thick.

7. Fire in dry H_2 (-50°C dewpoint) at 950°C for 10 minutes.

8. Fire in wet H_2 to oxidize the chromium at 900°C for 10 minutes.

9. Glass center rod with sufficient glass (7052) to make the entire bead.

10. Assemble the two parts in a glass lathe, using shaped graphite mandrels, one to hold the sleeve and rod in the correct position, the second to apply pressure to the glass to make a flat bead.

The resulting bead should be clear and free from bubbles, and the oxide color should be dark green. The quality of the bead can be checked by firing it in hydrogen at the temperature that will be used in a subsequent brazing operation. A good bead will be unchanged after this treatment, but any small bubbles present that escaped visual detection will become noticeable through their growth in size, sometimes to the point of producing a hole through the bead.

FIG. 20.--Construction of high-conductivity coaxial r-f seal.

Tests made on seals constructed according to this procedure indicated that they would carry 100-150 w cw, at 3,000 MC without noticeable heating.

The two parts comprising each of the r-f line center conductors were brazed together using Nioro* foil brazing alloy with a hydrogen-oxygen torch supplying the heat. A simple brass jig was used to hold the two parts in the proper position during the operation. After brazing, a 0.050-in. hole was drilled into each line at the corner, as shown in Fig. 21. The quartz rods that were fitted into these holes during final assembly were necessary to hold the center conductors while the coaxial seals were being placed on the r-f line.

Although satisfactory matches were obtained in the demountable tube by simply tapering the r-f lines in size and impedance between the structure and standard 3/8-in. lines, the combination of the glass dielectric in the seals and the quartz support rods in the S-185 tube degraded the matches considerably, and it was necessary to modify the center conductors. Because the two lines were of different lengths, different matching techniques were used, as indicated in Fig. 21.

The resulting gun-end VSWR with the internal termination is shown in Fig. 22. The insertion loss of the tube is shown in Fig. 23, and since the loss of the structure itself is less than 1 db, the loss is that of the coated ceramic plates used as the internal termination, as described in connection with the demountable tube.

C. ELECTRON GUN

The electron gun used in the S-185 tube was a standard laboratory item having an L-cathode 0.090 in. in diameter. The guns were originally designed to mount in 1-1/4 inch

---

*(Au:17.5, Ni:82.5) Proprietary alloy of the Western Gold and Platinum Works, San Francisco.

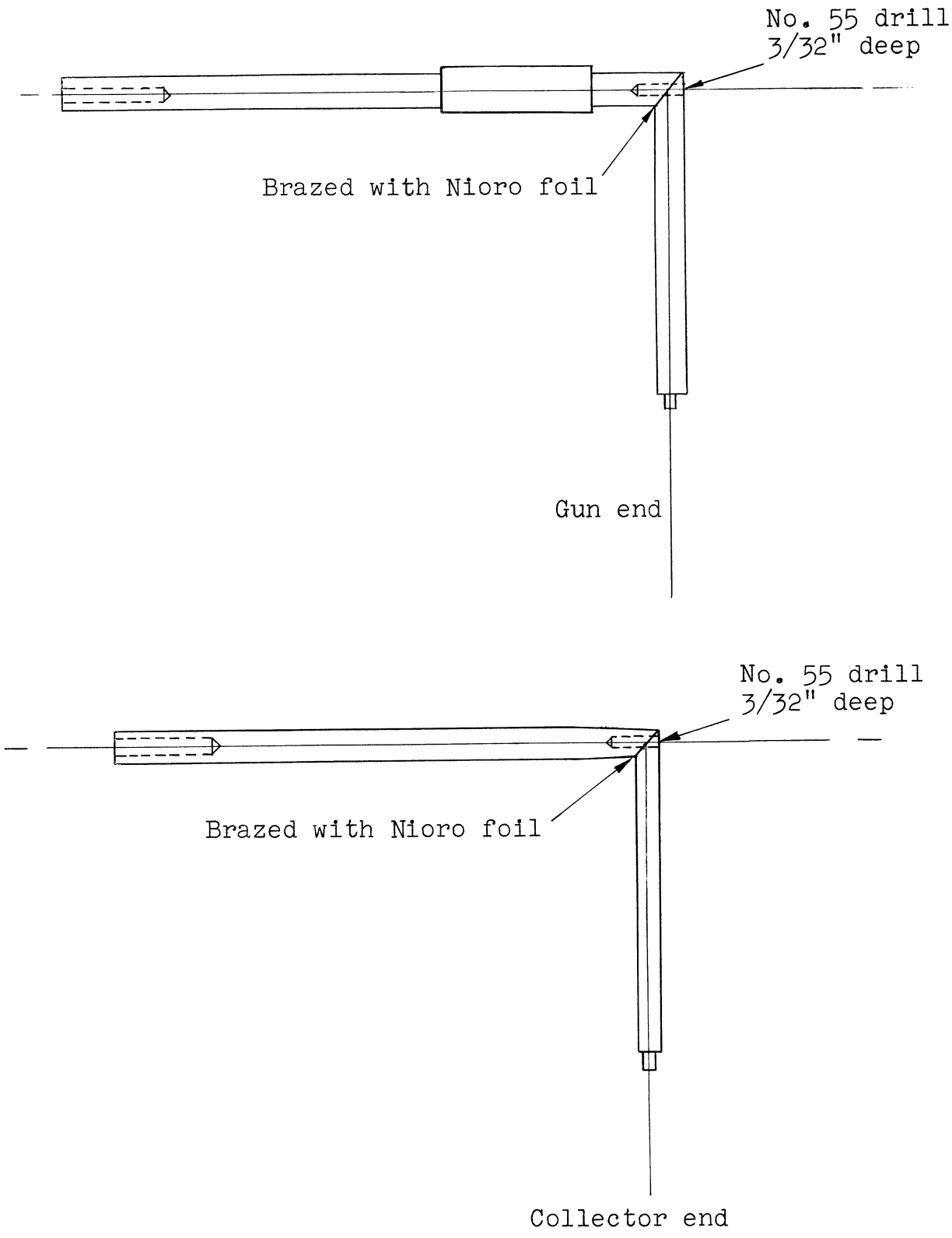

FIG. 21.--R-f line center conductors.

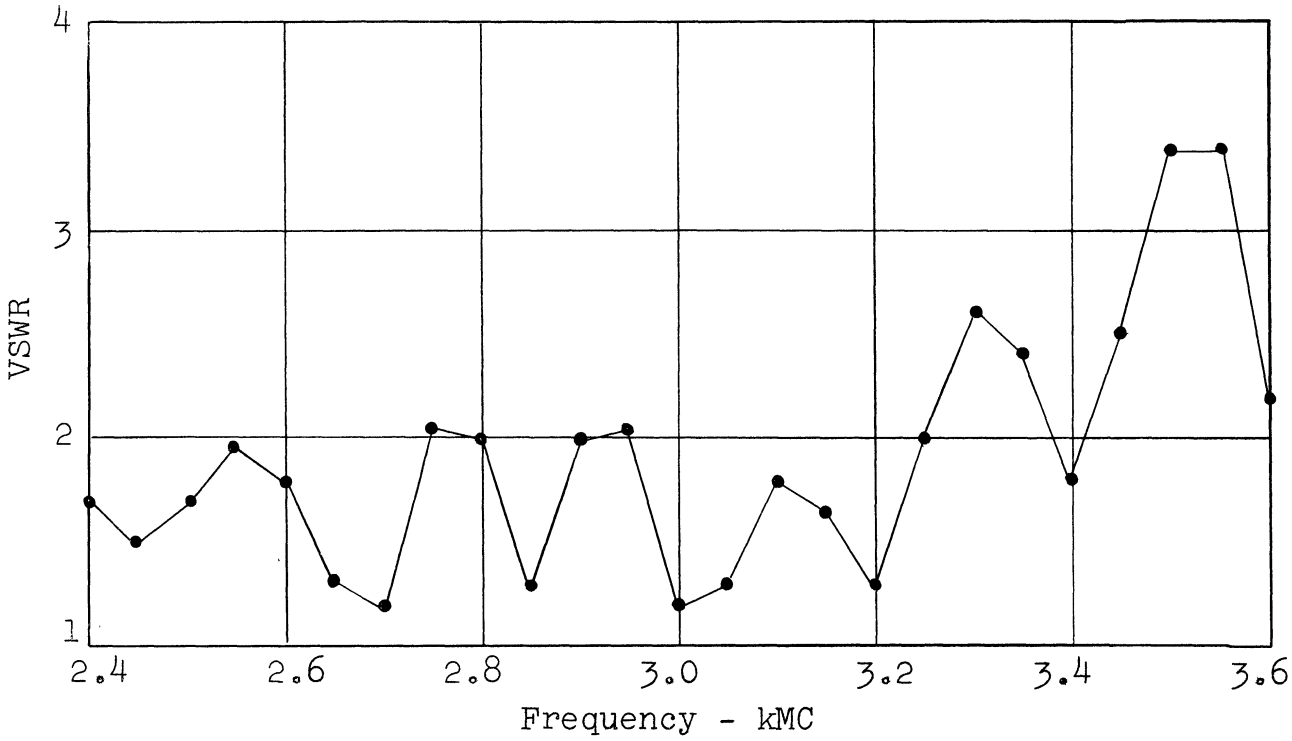

FIG. 22.--Gun-end match of tube S-185.

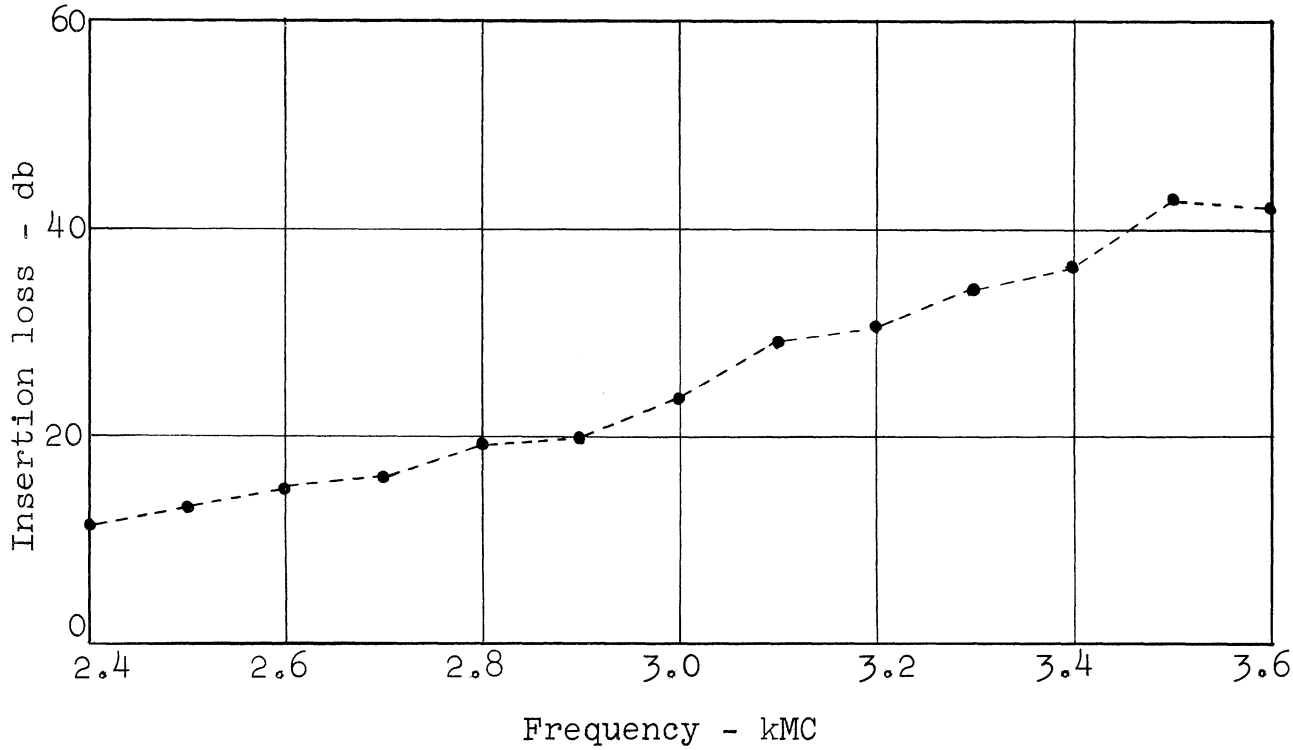

FIG. 23.--Insertion loss of tube S-185.

precision-bore glass using a three point suspension system made up of two ceramic "dumb bells" and a spring. Since the S-185 tube is of all-metal construction it was necessary to modify the mounting arrangement to permit use of larger insulators between the gun and its mounting cylinder, and to insulate the spring. The mounting arrangement used is shown in the assembly drawing of tube, Fig. 16. A drawing of the gun is shown in Fig. 24.

Although the maximum current density requirements for this tube were very high (approximately 6 a/cm^2), tests made with a diode using one of these guns indicated that a life of about 100 hours could be obtained.

D. COLLECTOR ASSEMBLY

Although the collector used in the S-182 tube performed satisfactorily, its construction required that water be supplied to it at a relatively high pressure to produce sufficient flow. A new water jacket was designed that reduced the input pressure requirement and was, in addition, easier to construct. Collector drawings are shown in Fig. 25. Assembly of the collector involved a step-brazing procedure which is outlined in Fig. 26.

In order to reduce the overall tube length to a minimum, and because the voltage insulation requirements were moderate (approximately 200 v) a coaxial Kovar-glass seal was developed for use at the collector. The seal assembly, as finally used, is compact and rugged; since the techniques used in its construction were new to this laboratory, they will be described here.

The powdered glass used for this seal is prepared in the following way:

1. Corning 7052 glass was ground to pass through a 20-mesh and collect on a 30-mesh sieve.

2. The powdered glass was boiled in dilute hydrochloric acid to remove iron contamination. (The only ball mill

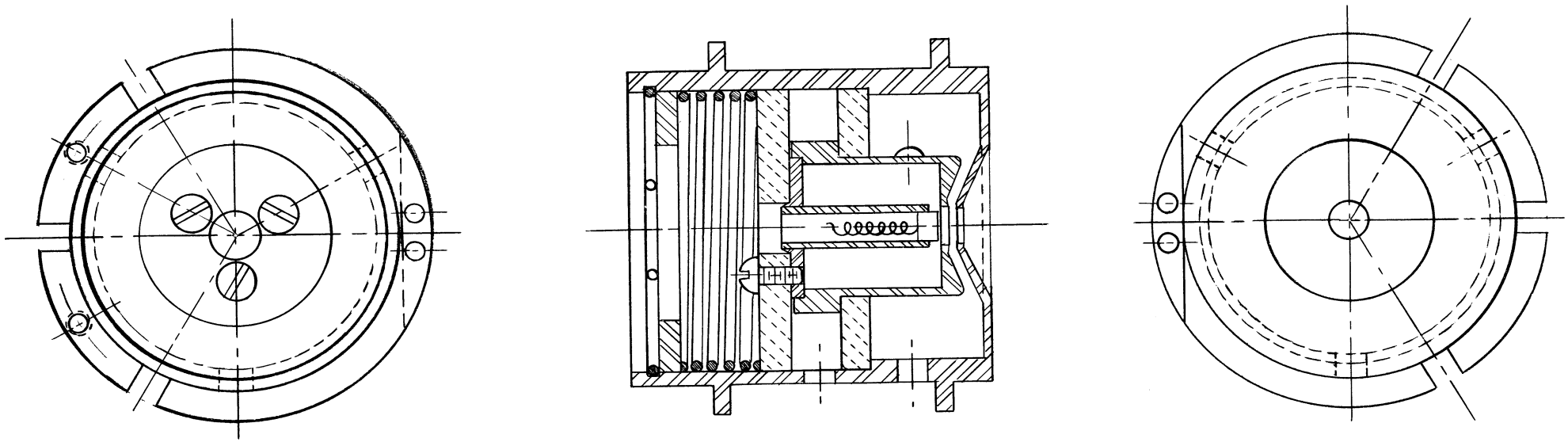

FIG. 24.--Electron gun for tube S-185.

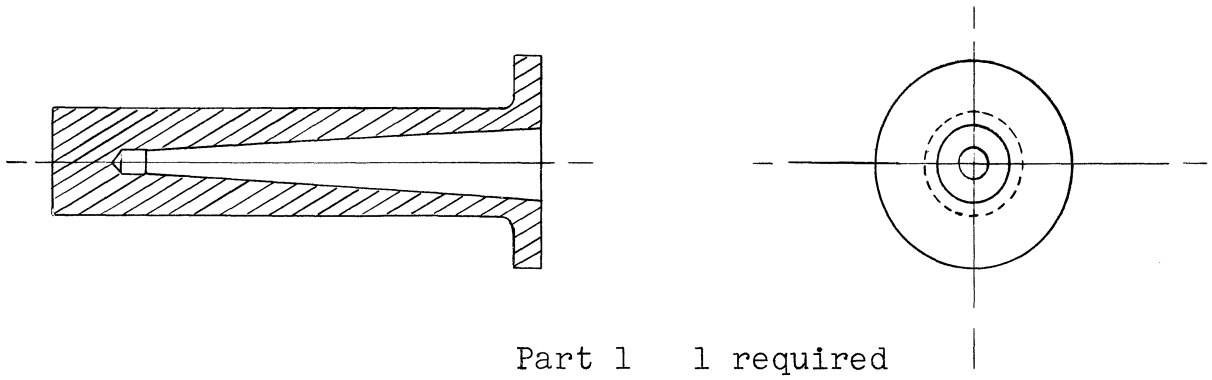

Part 1 1 required

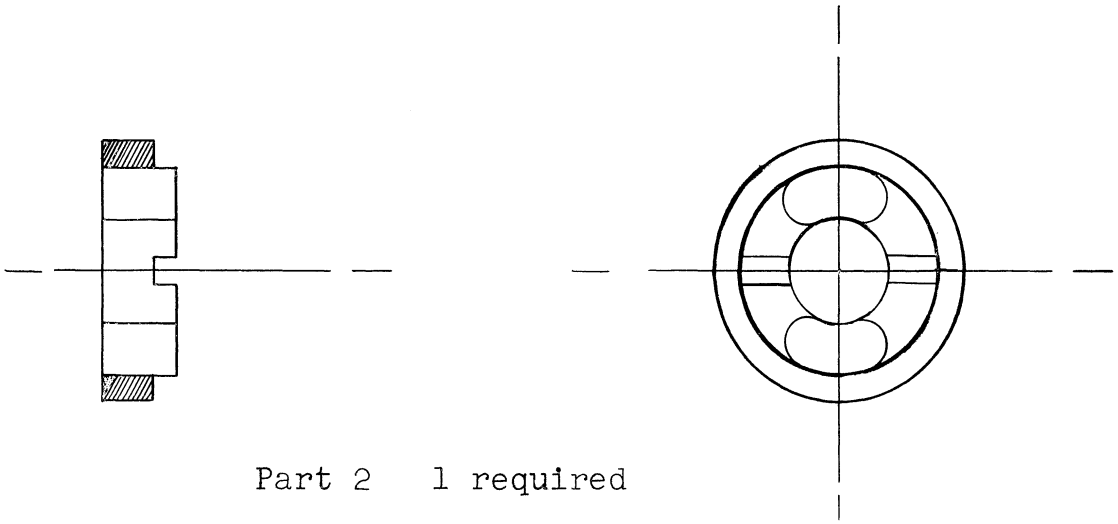

Part 2 1 required

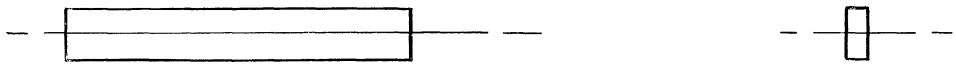

Part 3 2 required

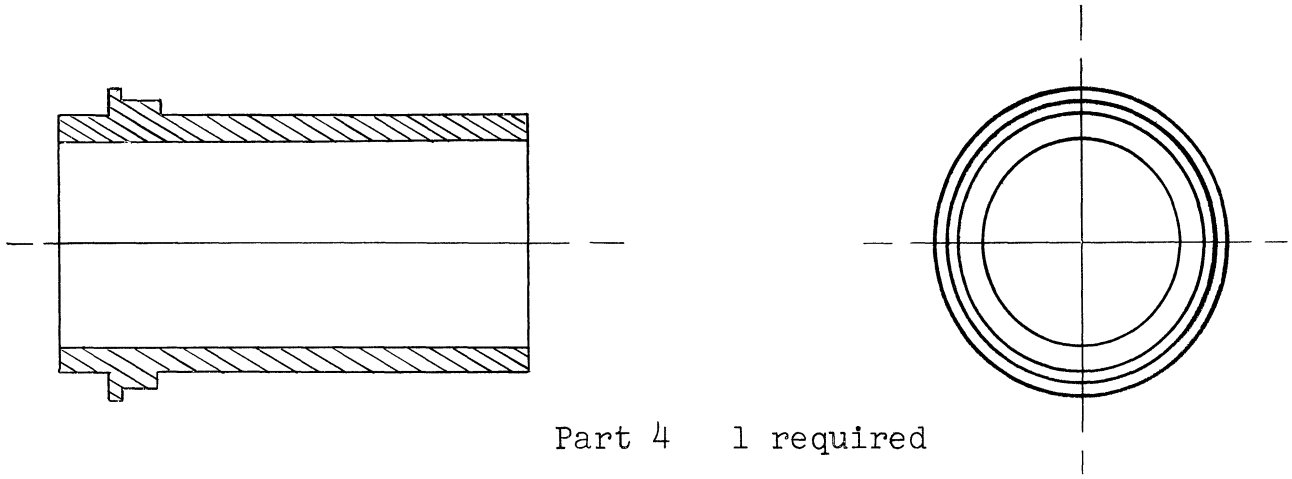

Part 4 1 required

FIG. 25.--Collector parts drawings.

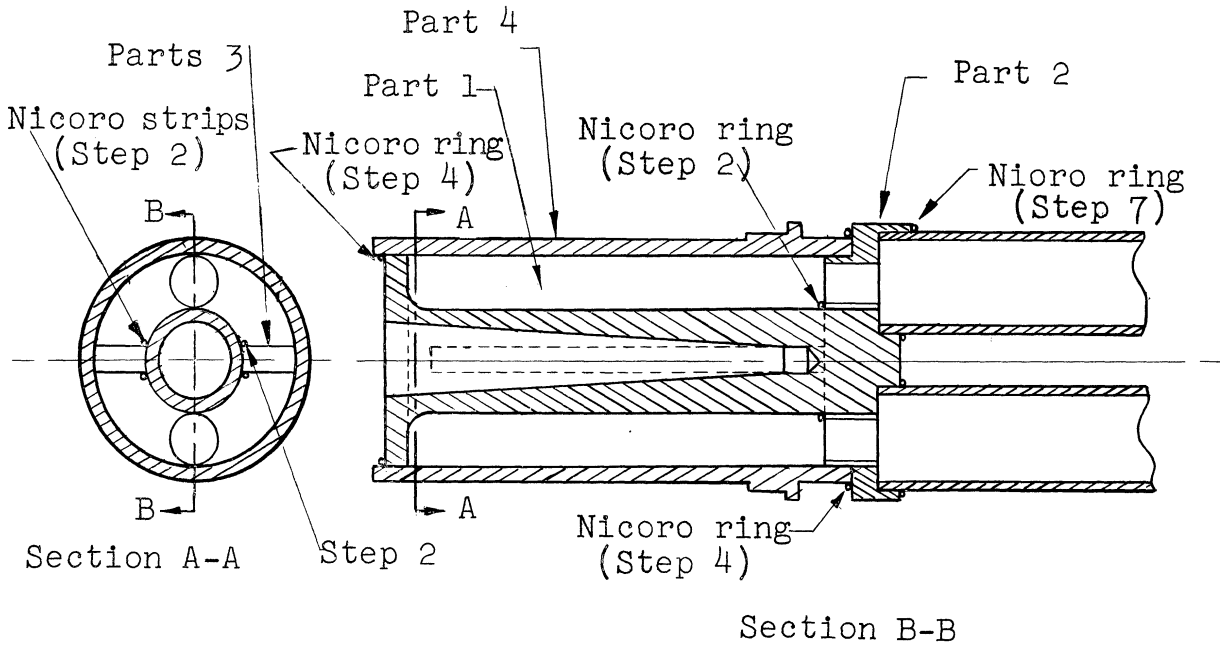

Assembly Procedure

1. Assemble Parts 1, 2, and 3. The free ends of the vanes, Parts 3, may be held during brazing with wire.

2. Braze in H_2 using Nicoro* alloy.

3. Shape outer edges of vanes so jacket, Part 4, can be placed in position.

4. Braze in H_2 using Nicoro alloy.

5. Counterbore 1/4" holes for water lines.

6. Insert water lines (each about 1" of 1/4" copper tubing).

7. Braze with Nioro alloy.

*Proprietary alloy of Western Gold and Platinum Works, San Francisco. (Au:35, Ni:3.0, Bal:Cu).

FIG. 26.--Assembly of collector.

available for the grinding was constructed of iron. The use of a porcelain ball mill would eliminate the contamination that results.)

3. The glass was washed thoroughly with distilled water with a final rinse in acetone.

4. The powdered glass was dried in hot air.

After this preparation, the powdered glass apparently could be stored for some time in a covered container. Just prior to use, the glass was treated according to the following schedule:

1. The glass was washed in dilute hydrofluoric acid (50 per cent by volume).

2. The glass was washed in distilled water with a final rinse in acetone.

3. The glass was dried in hot air.

4. The glass was transferred immediately to the jig assembly.

After machining and polishing, the Kovar sleeves were cleaned, degreased, and fired in wet hydrogen at 1000°C for 20 minutes, following normal procedures. The sleeves were then oxidized at 800°C for 20 minutes in air. In the experiments conducted here the oxidation was accomplished by using a gas-oxygen flame with the work rotating in a lathe. Since the quality of the finished seal is a function of the amount of oxide on the sleeve, more consistent results could be achieved by oxidizing the sleeves in a temperature-controlled oven as described by Pask.[10]

After the oxidation, the sleeves were transferred immediately to a graphite jig, as shown in Fig. 27. In order to produce a bead of sufficient thickness in this configuration, it was found necessary to completely fill the space between the sleeves with powdered glass. The whole assembly was heated in a nitrogen atmosphere at 975°C for ten minutes. The furnace was cooled at a rate of about 20°C per minute, held at 450°C for ten minutes, and then allowed to cool to room temperature.

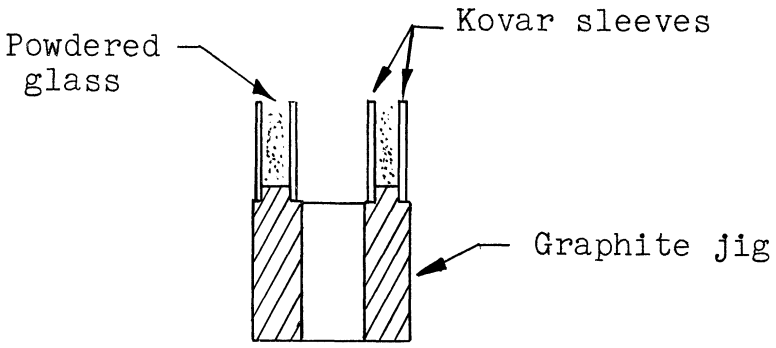

FIG. 27.--Construction of coaxial collector seal.

The glass in the resulting seal was clear, and the Kovar-glass interface had the normal gray color. The oxide was removed from the Kovar by electrolyzing the assembly in 20-percent hydrochloric acid, after which a flash plating of copper was applied to the sleeves.

The brazing of the seal to the collector and to the collector mounting flange was accomplished with the aid of a simple cylindrical graphite jig which served to support the three pieces in the proper position, without force, other than its own weight, being applied to the glass. This precaution was necessary to prevent deformation in the glass since the brazing temperature was near the softening point of the glass. The brazing alloy used was silver-copper eutectic, and the assembly was heated for approximately five minutes, or until the alloy flowed, in a hydrogen atmosphere at 800°C. The furnace was again cooled slowly to prevent strain formation in the glass. The completed collector assembly is shown in Fig. 28.

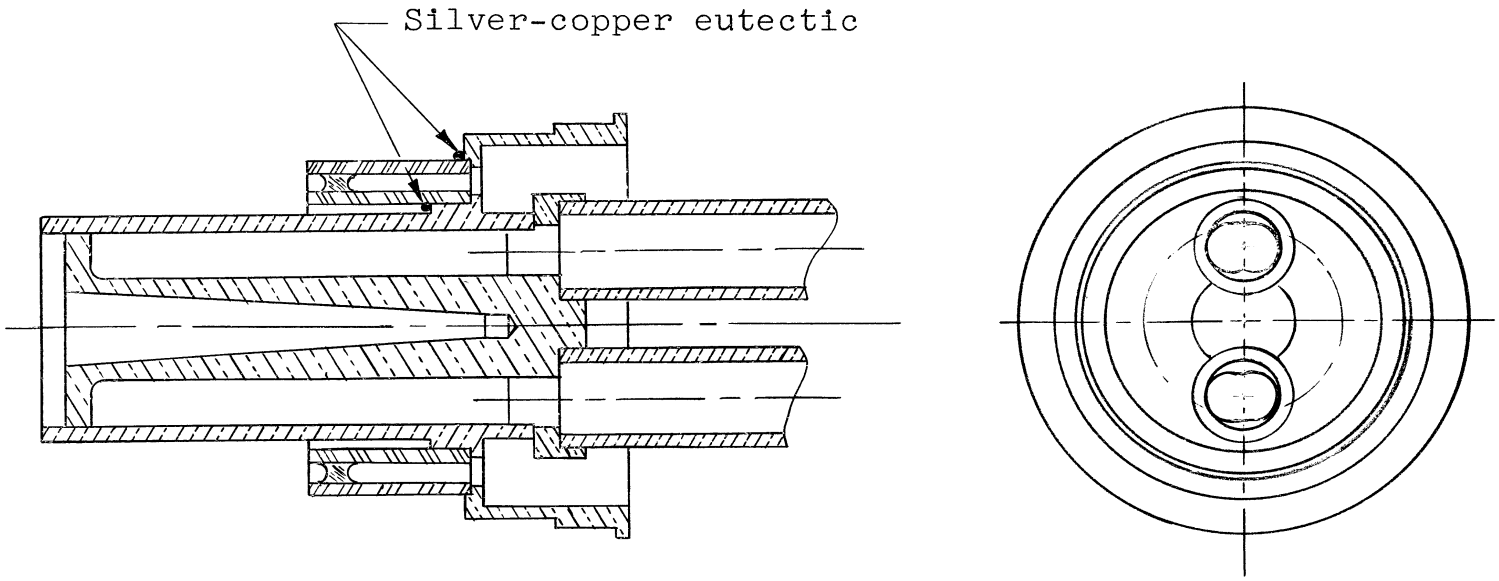

FIG. 28.--Complete collector subassembly.

III. TUBE ASSEMBLY

Construction of the tube was simplified by the use of step-brazing processes which made possible the elimination of several complicated jigs that would have been necessary if all the tube parts had been assembled in one operation. After the subassemblies described in the previous section were completed, the mating surfaces of the blocks, side plates, end bells, and r-f lines were silver-plated to a thickness of 0.0003 in. The parts were then assembled and bolted together, using stainless steel bolts. The ends of the center conductors of the r-f lines were held on their axes by simple cylindrical ceramic jigs. The whole assembly was heated in a hydrogen furnace at a temperature of about 800°C until the brazing alloy flowed. The brazing alloy in this operation is silver-copper eutectic, a thin interface layer of which is formed during the plating process.

After this assembly was leak-checked, the r-f beads were mounted at the ends of the r-f lines. A ring of 0.020 in. TAW (tantalum-tungsten alloy) was placed at the end of the slotted center conductor to insure good contact between it and the center conductor of the bead assembly. The brazing alloy used was Incosil 15* formed into a ring and placed adjacent to the joint in the outer conductor. A graphite jig was used to maintain alignment of the conductor of the bead during the brazing operation, since the flow point of the alloy is near the softening point of the glass. The tube was heated in hydrogen at about 700°C until the brazing alloy flowed. Cooling was done at a slow rate to prevent the formation of strains in the glass seals.

The ceramic loading plates, coated with "Aquadag" to a resistivity of about 300 ohms per square, were then installed,

---

*Proprietary alloy of the Western Gold and Platinum Works, San Francisco. (Cu:24; In:15; Bal:Ag)

and the r-f matches were checked. After determining that the matches and insertion loss characteristics were satisfactory, the collector was installed. The graphite jigs were again used on the r-f seals, and another such jig was used at the collector to take some of the weight of the collector off of the glass seal. Incosil 15 formed into a ring was again used as a brazing filler metal, and the tube was heated to about 700°C in hydrogen. If it were not necessary to check the matches and insertion loss, the collector and r-f seals could be installed in one operation.

The final seal on the tube was made at the gun end. After the gun and stem assembly was in position, the tube was mounted vertically in a hydrogen bell jar. A ring heater inside the copper cup holding the stem was used to heat the joint to the flow point of Incosil 15 alloy, which was placed as a ring adjacent to the joint. The gun-end r-f line and the glass in the stem assembly were protected by heat-shields during this operation.

IV. PROCESSING

Except in a few details, the processing of the 185 tube was carried out in the same manner as for any other tube. Since the tube is constructed almost entirely of copper, it was desirable to prevent, or at least retard, heavy oxidation of the tube during bake-out. Therefore, the tube was wrapped with aluminum foil, and a forming-gas line was introduced into this package. During bake-out an atmosphere of forming gas (5 per cent hydrogen, 95 per cent nitrogen) was maintained around the tube. A flow rate of about 10 cubic feet per hour was used. This procedure resulted in negligible oxidation of the tube surfaces. The tube was baked for about eight hours at 400°C.

The tube was connected to the glass manifold of the pumping station by means of a Kovar-glass seal, with a spare getter

placed in the glass part of the tubulation. After activation of the cathode, which followed normal procedure for L-cathodes, the tube was operated with a magnetic field in order to clean up the collector and parts of the r-f structure by electron bombardment.

The tube was sealed off in the glass part of the vacuum tubulation for several reasons. First, this procedure avoided the necessity for replacing the copper tubulation in case gun difficulties developed in the first few hours of operation. Also the getter which was placed inside the glass part of the tubulation gave a rough qualitative indication of vacuum conditions inside the tube. Finally, although a pinch off would be made in the copper tubulation if the tube performed satisfactorily, an operation of this kind with the tube connected to a glass manifold would be somewhat hazardous.

APPENDIX A: DESIGN OF FOLDED-LINE BACKWARD-WAVE OSCILLATORS

The basic structure considered in this analysis can be thought of as either an "interdigital" structure or a folded-strip transmission line. Since the latter concept has some advantages with regard to visualization of the interaction process, the "folded-line" designation is preferred. Figure A-1 shows the basic form of the structure and the notation used for dimensions.

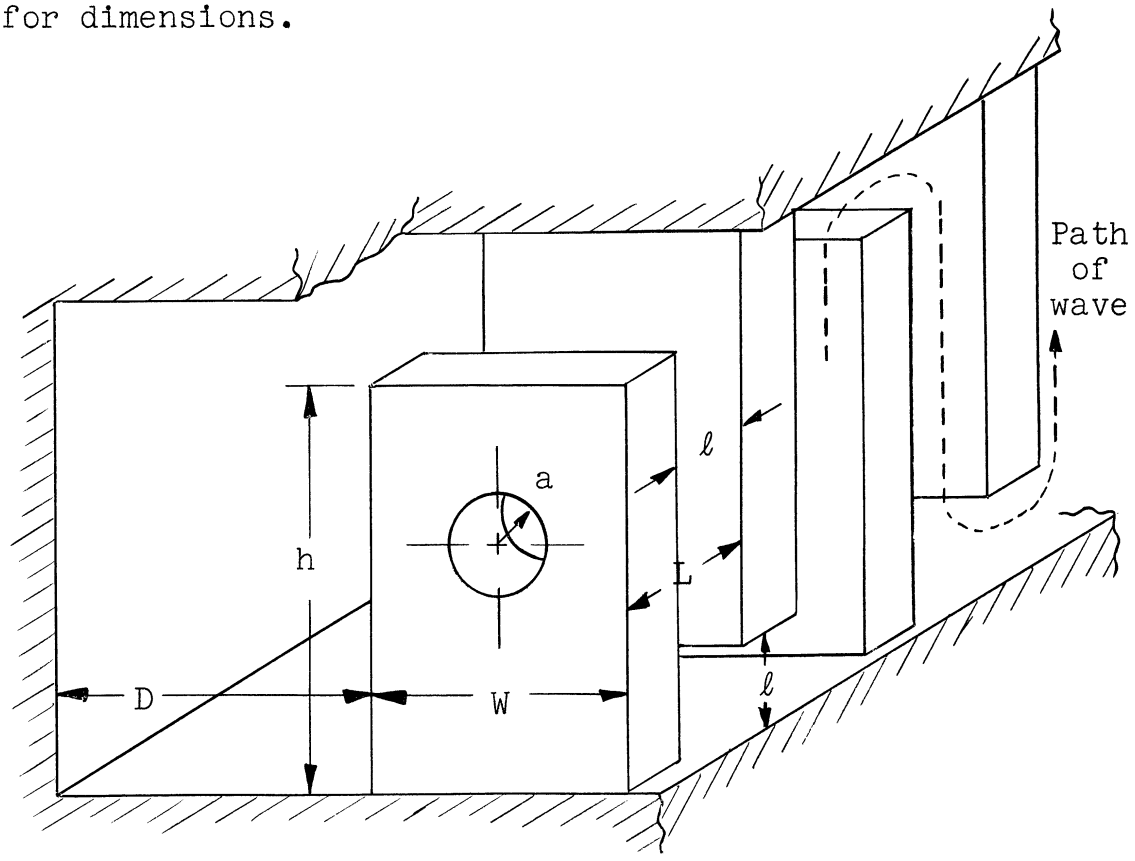

FIG. A-1.--The folded-line structure showing the notation used for dimensions.

In the following analysis, certain simplifying assumptions are made as follows: (1) The operating frequency is far enough

from any cut-off value so that the presence of side walls and periodic discontinuities owing to the bends has negligible effect on both the impedance of the structure and the velocity of the wave. The analysis is still valid for other cases, provided the proper values of impedance and velocity are used in the equations. (2) The value of the electric field at the edge of the hole is the same as that which would obtain with no hole (or a gridded hole). In cases where this assumption is obviously in error, a suitable adjustment can be made in the impedance, and the analysis carried out as before. If the diameter of the hole is not greater than one-third the smallest dimension of a "tooth" face, the above-stated condition probably holds very well. (3) The value of the gain parameter C is small (less than 0.1). This limitation is probably not too important since it is difficult to produce large values of C in microwave tubes which use space-harmonic structures.

It should be noted at the outset that the design of a backward-wave oscillator cannot be carried out in a straightforward manner, but requires several trials to bring all of the factors involved into agreement. For example, for a given frequency and voltage range, the power output may be insufficient due to limitations of beam perveance or beam density, necessitating a change in the choice of beam voltage. Again, since the efficiency of the tube is not known in advance, the beam current required to produce a certain power output may require a beam diameter which is incompatible with the size of the structure initially chosen. In the design procedure presented here, reasonable estimates (based on experience) of some of the unknown quantities are presented in order to shorten the trial-and-error process.

1. STRUCTURE DESIGN. The first step in the design is the choice of structure dimensions. The relationship between structure dimensions and operating frequency and voltage can be obtained by noting that the beam velocity must be near the phase velocity of the first backward-wave space-harmonic of

the circuit. If it is assumed that the r-f wave follows around the folds of the line with the velocity of light (experience indicates that this assumption is reasonable except near cut-off frequencies), the phase constant β of the desired backward-wave mode is given by

$$\beta = \frac{\omega}{v_{-1}} = \frac{2\pi \times \text{frequency}}{\text{velocity of first backward-wave mode}}$$

$$= \frac{2\pi}{\lambda_o}(1 + h/L) - \pi/L \qquad \text{(A-1)}$$

where λ_o is the free-space wavelength and the other quantities are defined in Fig. A-1. (For detailed derivation of Eq. (A-1), see reference 4). A corresponding "circuit" voltage V_{-1} can be defined as the accelerating voltage of an electron traveling at the backward-wave phase velocity:

$$\frac{V_{-1}}{256{,}000} = \left(\frac{v_{-1}}{c}\right)^2 = \left(\frac{2\pi}{\lambda_o \beta}\right)^2 \qquad \text{(A-2)}$$

where c is the velocity of light. Substituting for β,

$$V_{-1} = \left(\frac{1012}{\frac{\lambda_o}{L} - 2(1 + h/L)}\right)^2 \qquad \text{(A-3)}$$

Equation (A-3) is plotted in Fig. A-2 for various values of h/L. For a given value of V_{-1} (which will be less than the actual operating voltage V_o by perhaps 2 - 20 per cent), the value of L/λ_o can be read off directly and the dimension L determined. Since L/λ_o is proportional to frequency for a fixed L, the complete tuning curve of a given structure can also be found from Fig. A-2. Of course, the particular tuning curve

will depend on the choice of h/L, and here some judgment is needed. As shown by the curves of Fig. A-2, small values of h/L result in a minimum voltage range to cover a given frequency range. However, considerations of line size and proportion, including the need for a suitable hole for the beam and a reasonable value of characteristic impedance, limit the practical values of h/L to something greater than 2. A fairly good starting value is h/L = 3, but several trials may be needed to determine the best value for the desired beam size and voltage and frequency range.

An upper limit to the value of h/L is imposed by the high-frequency cut-off of the structure. Owing to reflections from the corners, a high-frequency cut-off will occur at a frequency somewhat lower than that for which the distance between corners is one-half wavelength. If, in addition, the teeth are not perfectly spaced but have alternate wide and narrow gaps between them, a stop band may occur at half the above frequency. This limits the sum of h and L to about a quarter wavelength, or

$$\frac{L}{\lambda}\,(1 + h/L) < 1/4 \qquad \text{(A-4)}$$

This limit is indicated by the dashed line of Fig. A-2.

Having determined L and h, the remaining dimensions ℓ, W, D, and the tube length must be chosen. In general, the gap length ℓ is made as large as possible consistent with mechanical and heat conduction requirements of the teeth. The width W, together with ℓ, determines the characteristic impedance Z_o of the line for matching purposes:

$$Z_o \simeq 377\,\frac{\ell}{W + \ell} \qquad \text{(A-5)}$$

In Eq. (A-5), the effective line width W + ℓ is used instead of W to account for fringing fields at the edges of the teeth. This approximation appears to be in good agreement

with observed results. For best matching into 50-ohm coaxial lines, W should be about 6.5 ℓ, but higher values of Z_o can be used. If W is less than 3 ℓ, the folded-line approximations probably do not apply too well.

The distance to the side wall D determines the low-frequency cut-off of the structure, and should be chosen so that the lowest operating frequency is at least 50 per cent higher than this cut-off. The low-frequency cut-off is approximately that frequency for which the inductance per unit length of the side section resonates with the capacitance per unit length of the teeth. The plot shown in Fig. A-3 can be used to determine the dimension D for a given cut-off frequency.

2. CALCULATION OF C. In order to determine the length of the structure and the power output, it is necessary to evaluate the gain parameter C. Using the analysis and notation of Pierce,[5] C is given by the following expression: (for a complete derivation, see reference 4)

$$C^3 = \frac{V^2 M^2 I_o}{8V_o(\beta L)^2 P} \qquad \text{(A-6)}$$

where V is the peak circuit voltage appearing across the interaction gaps at the edge of the hole for a given total transmitted power P, V_o and I_o are d-c beam voltage and current, respectively, and the phase constant β is given by Eq. (A-1).

The factor M in Eq. (A-6) is a "gap coefficient" which takes into account the reduction in effectivenss of the r-f field on account of both the transit time of the electrons across the gap and the fact that the r-f field is not uniform over the cross-section of the beam.

$$M = \frac{\sin \frac{\beta\ell}{2}}{\frac{\beta\ell}{2}} \sqrt{R_1} \qquad \text{(A-7)}$$

where R_1 is a reduction factor computed by averaging V^2 over the beam cross-section. (See reference 6).

$$R_1 = \frac{2}{r^2}\int_0^r \frac{I_o^2(\gamma\rho)}{I_o^2(\gamma a)}\,\rho d\rho$$

$$= \frac{I_o^2(\gamma r) - I_1^2(\gamma r)}{I_o^2(\gamma a)} \qquad \text{(A-8)}$$

where I_o and I_1 are modified Bessel functions and γ is given by

$$\gamma^2 = \beta^2 - (\omega/c)^2 \qquad \text{(A-9)}$$

(For slow waves, γ is approximately equal to β.)

The factor M can be expressed as a function of β, γ, ℓ, the beam radius r, and the ratio of the beam radius to hole radius, a. If it is assumed that $\gamma \simeq \beta$, values of M can be obtained from Fig. A-4. Enter the chart of Fig. A-4 with values of V_{-1} as determined from Fig. A-2, project both ways to the proper values of r/λ_o and ℓ/λ_o given on the diagonal lines, project up to the curves and then toward the center to the reference lines. The value of M is read from the alignment chart at top center. The value of βr, as given in the left-hand section, should be noted for use in later computations.

Equation (A-6) may be put into a more useful form if it is assumed that $V^2/2P$ is the ordinary characteristic impedance of a strip transmission line as given by Eq. (A-5). This approximation should be very good for $W > 3\ell$. Then, if a beam propagation constant β_e is defined as

$$\beta_e = \frac{\omega}{u_o} = \frac{2\pi\ 506}{\sqrt{V_o}\ \lambda_o} \qquad \text{(A-10)}$$

where u_o is the d-c beam velocity, the expression for C can be put into the form:

$$C^3 = \frac{2.47\times10^{-8} Z_o M^2 (\beta_e/\beta)^2 I_o}{(L/\lambda_o)^2} \qquad \text{(A-11)}$$

All of the factors of Eq. (A-11) can be found from Eqs. (A-3), (A-5), (A-7), and the circuit dimensions (or the appropriate charts) except β_e/β. Since β_e/β seldom exceeds 1.15, except for very high power tubes, this factor can be considered to be unity initially, and a correction made later if desired.

3. SPACE-CHARGE EFFECTS. For most practical tubes, space-charge effects are important in determining the required tube length, the power output, and the shift in operating frequency with beam current (frequency pushing). The evaluation of space-charge effects presented here is based on the work of Harman[7] and Grow.[1]

For purposes of this analysis, the space-charge parameter ω_q/ω appears to be more natural than the usual QC of Pierce. The relationship between the two is given by[1]

$$4QC \simeq \left(\frac{\omega_q}{\omega C}\right)^2 \qquad \text{(A-12)}$$

In Eq. (A-12), ω_q is the reduced electron plasma radian frequency, ω is the operating radian frequency, and C is the gain parameter given by Eq. (A-11). In terms of the beam and circuit parameters,

$$\omega_q = 7.96\times10^{10}\left(\frac{I_o}{u_o}\right)^{1/2} \frac{R_\omega(\beta r, r/a)}{r} \qquad \text{(A-13)}$$

where R_ω is a plasma frequency reduction factor depending on the beam and circuit parameters.[1,7] Equation (A-13) is not convenient for computation because of the dependence of the operating beam voltage (or u_o) on ω_q. For large values of ω_q/ω, (large space-charge), the ratio of beam velocity to circuit velocity is approximately equal to $1 + \omega_q/\omega$ (see reference 7). Using this relationship and Eq. (A-2), the relationship between ω_q/ω and the beam and circuit constants can be expressed as

$$\left(\frac{\omega_q}{\omega}\right)^2\left(1 + \frac{\omega_q}{\omega}\right) = 3.03\times10^4 \frac{I_o}{V_{-1}^{3/2}} F_1(\beta r, r/a) \qquad \text{(A-14)}$$

where

$$F_1 = \frac{R_\omega^2}{(\beta r)^2} \qquad \text{(A-15)}$$

The function $F_1(\beta r, r/a)$ is plotted in Fig. A-5 together with an alignment chart for determining ω_q/ω. The values of βr for use in Fig. A-5 can be found from the left-hand side of Fig. A-4.

4. OPERATING VOLTAGE. The actual operating voltage corresponding to a circuit voltage V_{-1} can be obtained by using the value of the velocity parameter b, plotted in Fig. A-6.

$$\frac{V_o}{V_{-1}} = \left(\frac{\beta}{\beta_e}\right)^2 = \left(\frac{u_o}{v_{-1}}\right)^2 = (1 + bC)^2 \qquad \text{(A-16)}$$

This relationship is also presented in the alignment charts of Fig. A-6.

Having obtained an estimate of V_o/V_{-1}, the tuning curves can be recalculated, if necessary, and some adjustment made

in the structure dimensions if a particular operating voltage is desired. If the value of ω_q/ω as found from Fig. A-5 is greater than 0.05, the value of C should be corrected also, and the entire design rechecked for the new value of C. The operating voltage does not depend on circuit loss to any great extent.

5. TUBE LENGTH. The necessary length of interaction structure can be estimated from the values of CN_{start}, plotted in Fig. A-6. The quantity N_{start} is defined as the number of beam wavelengths necessary to start oscillation at the value of C being used. The start-oscillation length is related to N_{start} by

$$\text{Length}_s = \frac{2\pi N_{start}}{\beta_e} = \frac{\lambda_o \sqrt{V_o}\, N_{start}}{506} \qquad \text{(A-17)}$$

The right-hand side of Fig. A-6 is an alignment chart for finding the starting length in terms of free-space wavelength, from appropriate values of CN_{start}, C, and V_o. Experience indicates that the actual active length of the tube should be from 1.5 to 2 times the starting length, low-power tubes being in general relatively longer than high-power tubes. If an internal termination is used at the collector end, additional length will be needed. For moderate circuit loss (up to 15 db or so), the indicated length should be multiplied by a factor 1 + (db loss)/45.

6. EFFICIENCY AND POWER OUTPUT. The best available estimate of backward-wave oscillator efficiency is that presented by Grow.[1] The theoretical relationship between efficiency and the space-charge parameter ω_q/ω, as presented in Fig. A-6, seems to predict the power output of practical tubes quite accurately. The "unadjusted" efficiency η_o can be found from Fig. A-6 by multiplying the plotted value of η_o/C by C. This can be done with the aid of the alignment chart at the left-hand side of Fig. A-6. The actual tube efficiency η is

found by multiplying η_o by a reduction factor depending on βr. This reduction factor is plotted in Fig. A-7 and is also incorporated in the alignment chart of Fig. A-6.

The power output is given by the product of efficiency and d-c beam power. For a fixed frequency, the power output varies approximately as the 3/2 power of beam current for large space-charge conditions ($\omega_q/\omega > 1.5C$), or as the 4/3 power of beam current for small space-charge conditions. The presence of circuit losses will reduce the power output from the value above. For moderate circuit losses, the reduction in db will be approximately one-half the circuit loss in db.

When designing a tube for a particular power output, limitations imposed by permissible cathode current density and maximum beam perveance[8] should be kept in mind.

7. CALCULATION OF STARTING CURRENT. One of the parameters of a BWO, which is of some interest, is the starting current, or the beam current at which oscillations just begin. For a structure of given dimensions, the starting current can be calculated from Eqs. (A-11), (A-16), (A-17), and the values of CN_{start} given in Fig. A-6. This may be a tedious process, however, because of the dependence of both C and N on V_o, which in turn depends on C and b.

For purposes of computing starting currents, it is convenient to redefine all quantities in terms of parameters which do not depend on beam current. A space-charge parameter Q' can be calculated from circuit constants alone, as follows:

$$Q' = \alpha Q = \left(\frac{v_{-1}}{u_o}\right)\left(\frac{QC}{C}\right) = \left(\frac{v_{-1}}{u_o}\right)\left(\frac{\omega_q}{\omega}\right)^2 \frac{1}{4C^3} \qquad \text{(A-18)}$$

Using Eqs. (A-11), (A-13) and (A-15),

$$Q' = \frac{7.55 \times 10^3 F_1}{K\, V_{-1}^{3/2}} \qquad \text{(A-19)}$$

where F_1 is found from Fig. A-5, V_{-1} is given by Eq. (A-3), and

$$K = \frac{2.47 \times 10^{-8} Z_o M^2}{(L/\lambda_o)^2} \qquad \text{(A-20)}$$

It is also necessary to have a first approximation to C, given by

$$C_1^3 = KI_o \qquad \text{(A-21)}$$

and a "circuit" N, or the number of wavelengths on the cold circuit:

$$N_c = \frac{506}{\sqrt{V_{-1}}} \left(\frac{\text{length}}{\lambda_o} \right) \qquad \text{(A-22)}$$

From the known relationships between CN, Q/N, and α at start-oscillation,[3,7] a new set of relationships between C_1, N_c and Q' can be derived (for the no-loss case) such that the starting current can be solved for explicitly. The plot of Fig. A-8 shows $C_{1(\text{start})}$ as a function of Q' with N_c as a parameter. The starting current is obtained from $C_{1(\text{start})}$ by use of Eq. (A-21). For moderate circuit losses, the starting currents will be increased approximately by a factor $(1 + \frac{\text{loss in db}}{45})^3$.

8. EXAMPLE. The following sample calculations taken from the design of Stanford Tube Type S-182-A are presented to illustrate the use of the design procedure. The requirements of this tube were:

tuning range: 2500 to 3500 MC
power output: 100 w cw

(1) Structure design. The structure design depends largely on the beam voltage, which in turn is determined by the probable efficiency and maximum obtainable beam perveance,

or current density. For Tube S-182-A, a beam voltage of about 3000 v at 3 kMC was desired because of available guns and power supplies. From Fig. A-2, the value of L/λ_o for this voltage and frequency is 0.035 for $h/L = 4$, or $L = 0.138$ in., $h = 0.550$ in. For simplicity, L was actually made 0.140 in. and $h = 0.600$ in. For mechanical reasons, the teeth were made 0.060 in. thick, leaving $\ell = 0.080$ in. For a line impedance of about 65 ohms, a width $W = 0.385$ in. was needed, the actual value used being $W = 0.400$ in. The transverse dimension D was made 0.600 in. corresponding to a low-frequency cutoff of 840 MC. (A smaller value of D could have been used.) The electron gun for this tube had a cathode diameter of 0.090 in., so the hole diameter was made 0.125 in.

(2) Calculation of C. From the dimensions given above, the following quantities can be computed:

$$L/\lambda = 0.0356$$
$$h/L = 4.3$$
$$\ell/\lambda = 0.0204$$
$$r/\lambda = 0.0114$$
$$r/a = 0.72$$
$$Z_o = 63 \text{ ohms}$$

From Eq. (A-3) or Fig. A-2, $V_{-1} = 3350$ v. (The voltage tuning range is 2100 to 5650 v and the highest frequency is below the possible high-frequency cutoff indicated in Fig. A-2.) From Eqs. (A-2), (A-7) and (A-8) or Fig. A-4, the following values are found:

$$\beta r = 0.625$$
$$\beta \ell = 1.11$$
$$M = 0.835$$

Using these values, C_1 (first approximation neglecting variation with beam voltage) is found to be $0.098\ I_o^{1/3}$. At an estimated 10-percent efficiency, a beam current of 300 ma would be needed, making $C_1 = 0.0655$.

(3) Space-charge parameter. From Fig. A-5, ω_q/ω is found to be 0.108 making $\omega_q/\omega C = 1.65$ (first approximation).

(4) Operating voltage. From Fig. A-6, $V_o/V_{-1} = 1.24$, or $V_o = 4150$ v. This ratio of operating to circuit voltage is not negligible in computing C, so a second approximation gives

$$C = \frac{0.0655}{(1.24)^{1/3}} = 0.061$$

$$\frac{\omega_q}{\omega C} = 1.77$$

$$V_o/V_{-1} = 1.24, \quad V_o = 4150 \text{ v}$$

(5) Tube length. From Fig. A-6, the starting value of N is 7.6, which for an operating voltage of 4150 v corresponds to a length of 0.965 wavelengths. This value makes the starting length 3.8 in., or the minimum operating length 1.5 x 3.8 = 5.7 in. (Actually, the minimum length should be computed at the high-frequency end of the range, since the tube is electrically shortest there. The actual tube was made approximately 6-1/2 in. long.)

(6) Efficiency and power output. From Fig. A-6, the "unadjusted" efficiency η_o is 0.107, which after applying the reduction factor of Fig. A-7 gives an efficiency η of 9.75 per cent. The power output is then 121 w, based on the calculated operating voltage. (The actual operating voltage and corresponding power output will usually be somewhat smaller than calculated on account of the error in assuming that the wave propagates at the "geometric" velocity.) Assuming that the power output varies as $I_o^{3/2}$, a beam current of about 265 ma should give 100 w output.

(7) Starting current. For a tube length of 6-1/2 in., $N_c = 14.3$, $K = 9.5 \times 10^{-4}$, $Q' = 11.5$. $C_{1(start)}$ is found to be 0.0255, giving a starting current of 17.5 ma.

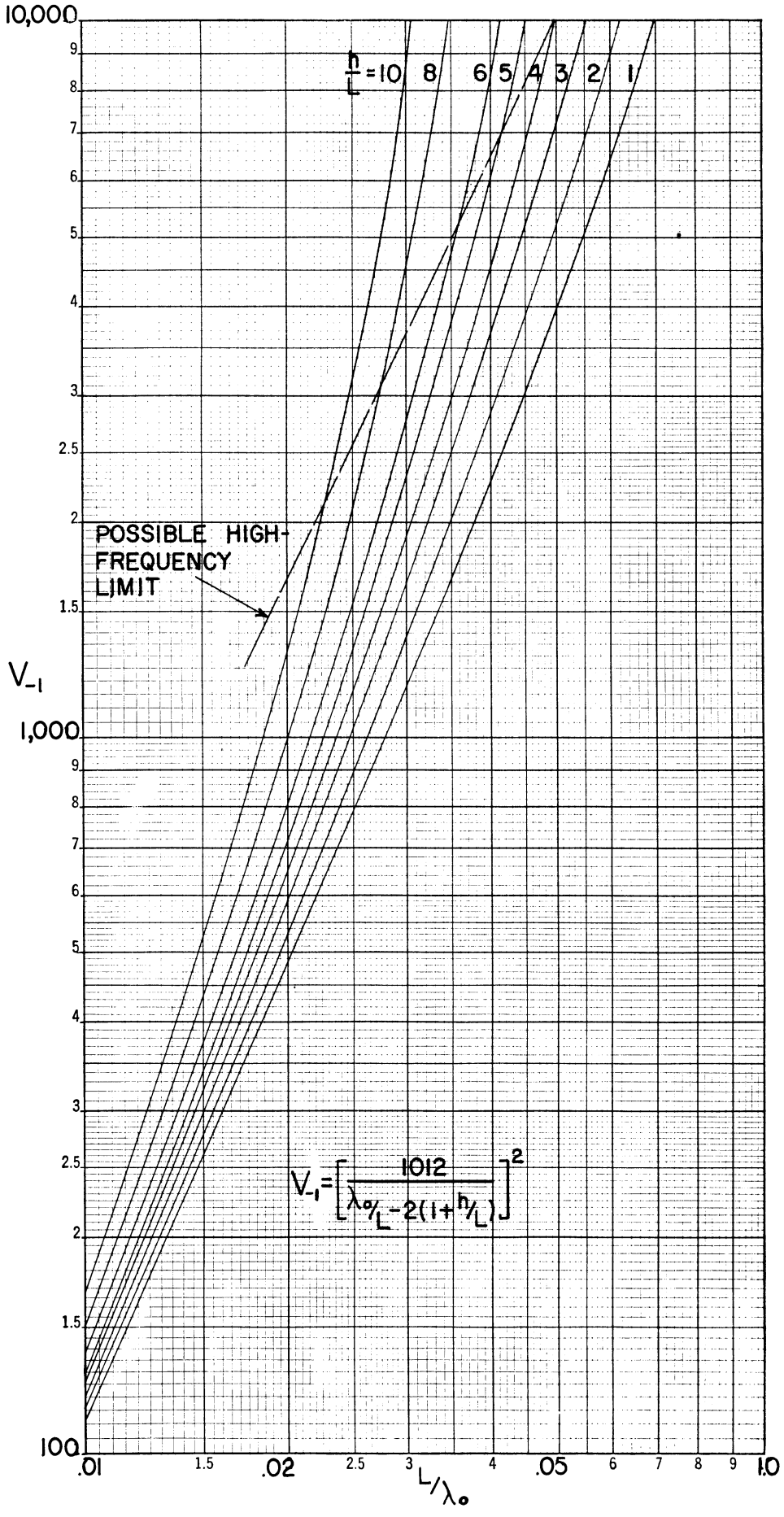

FIG. A-2.--Universal tuning curves for a folded-line BWO.

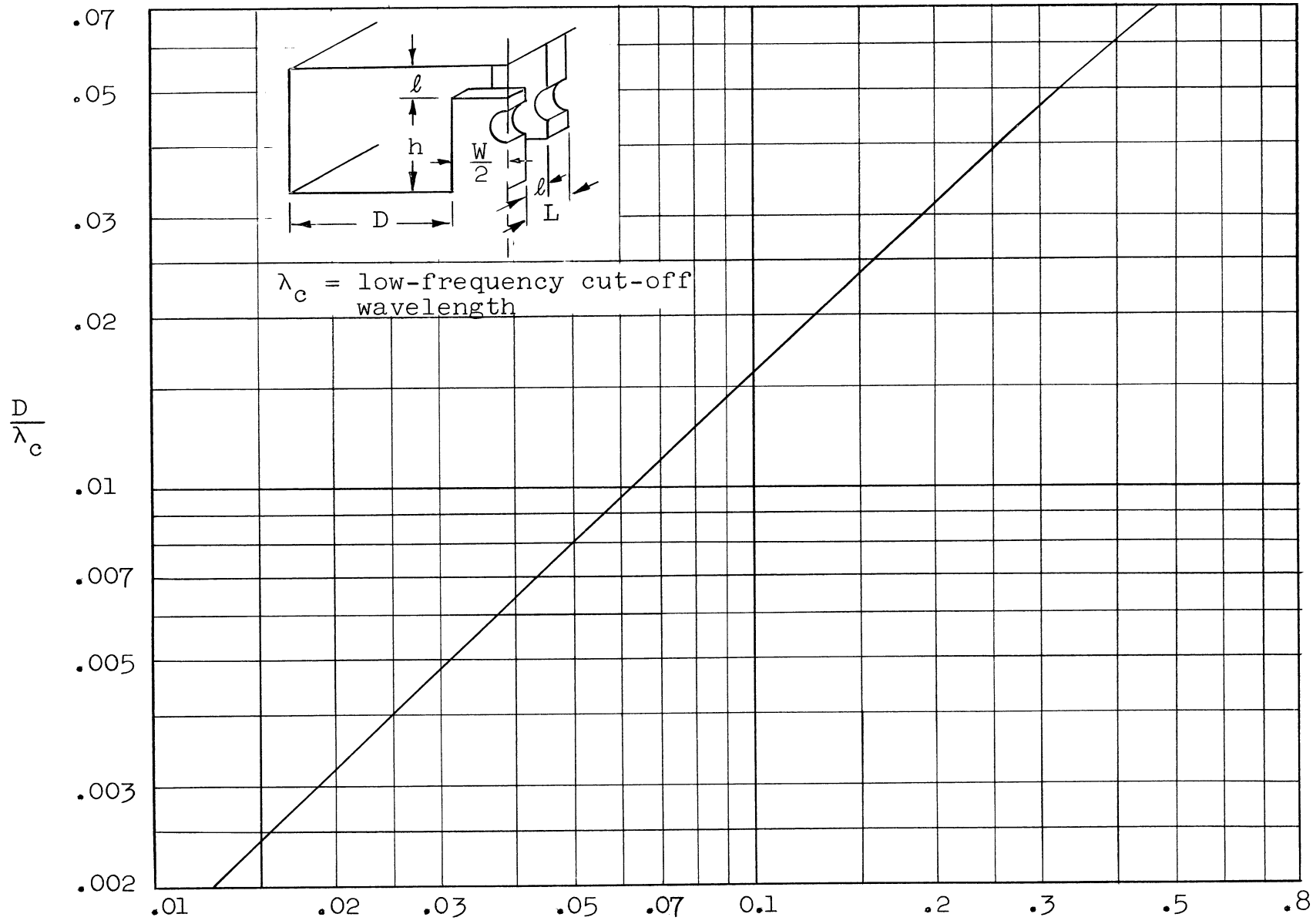

FIG. A-3.--Relationship between dimensions and low-frequency cut-off for a folded-line structure.

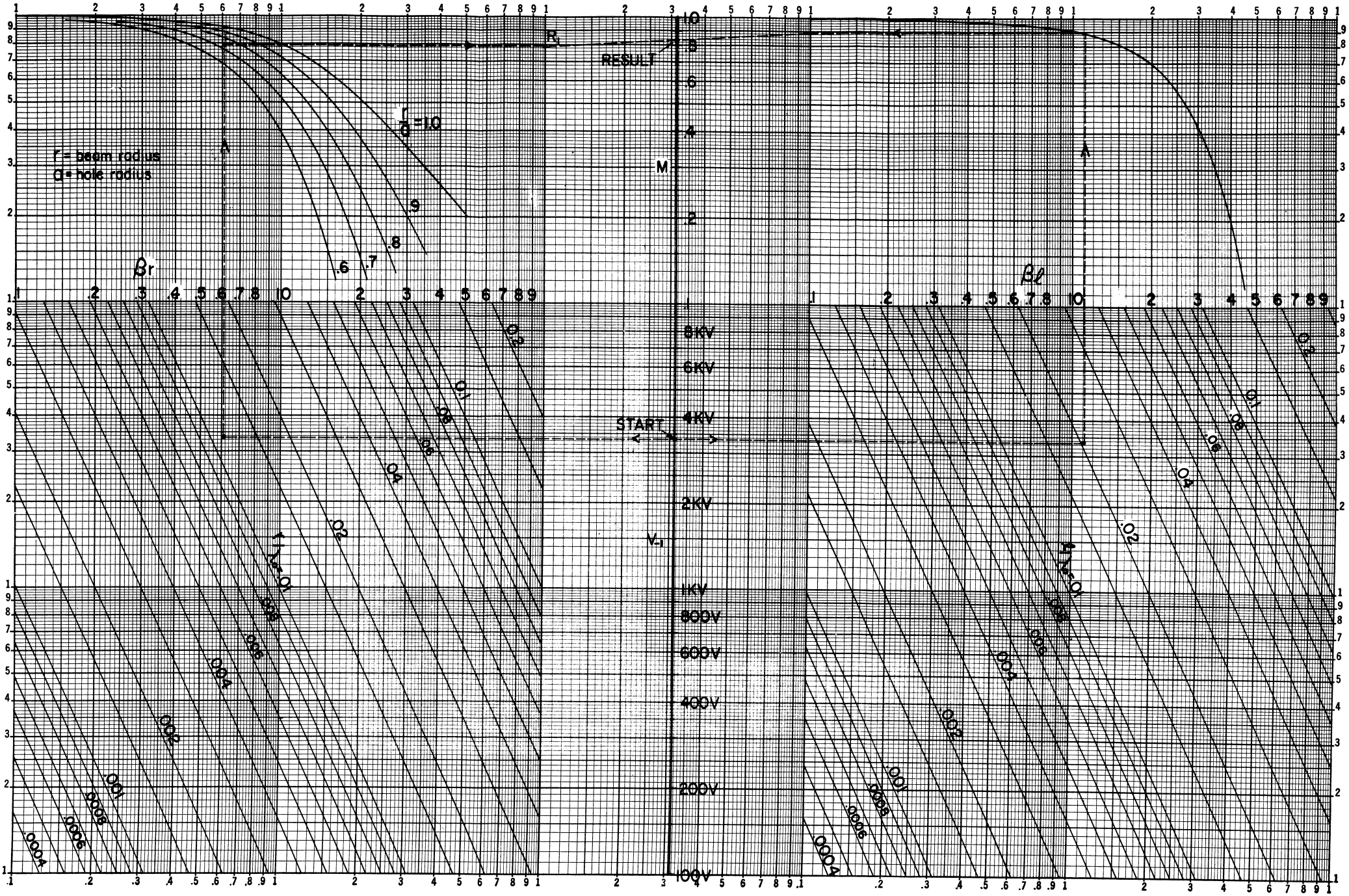

FIG. A-4.---THE FACTOR M FOR USE IN EQ. (A-11).

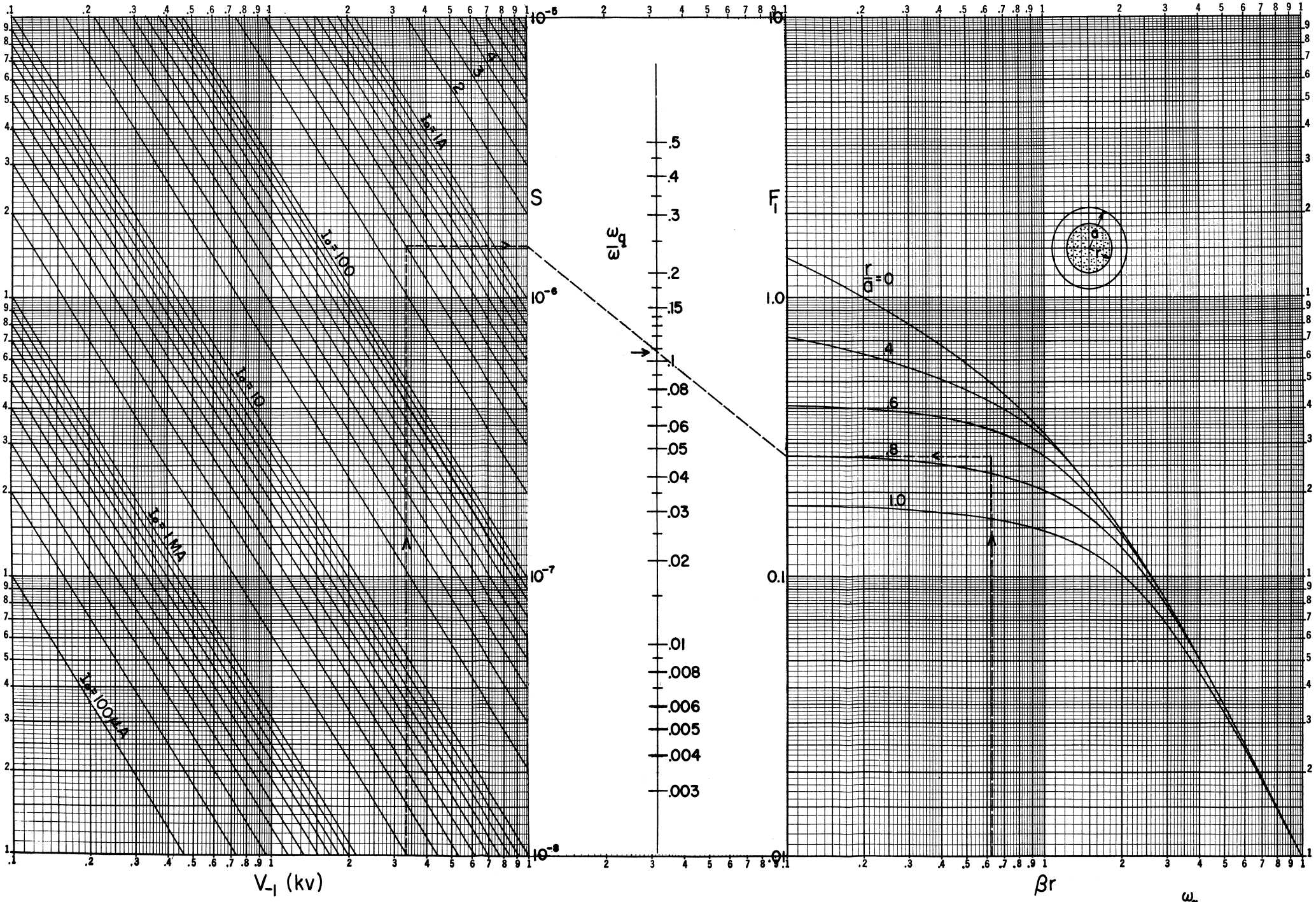

FIG. A-5.--SPACE-CHARGE PARAMETER $\frac{\omega_q}{\omega_l}$.

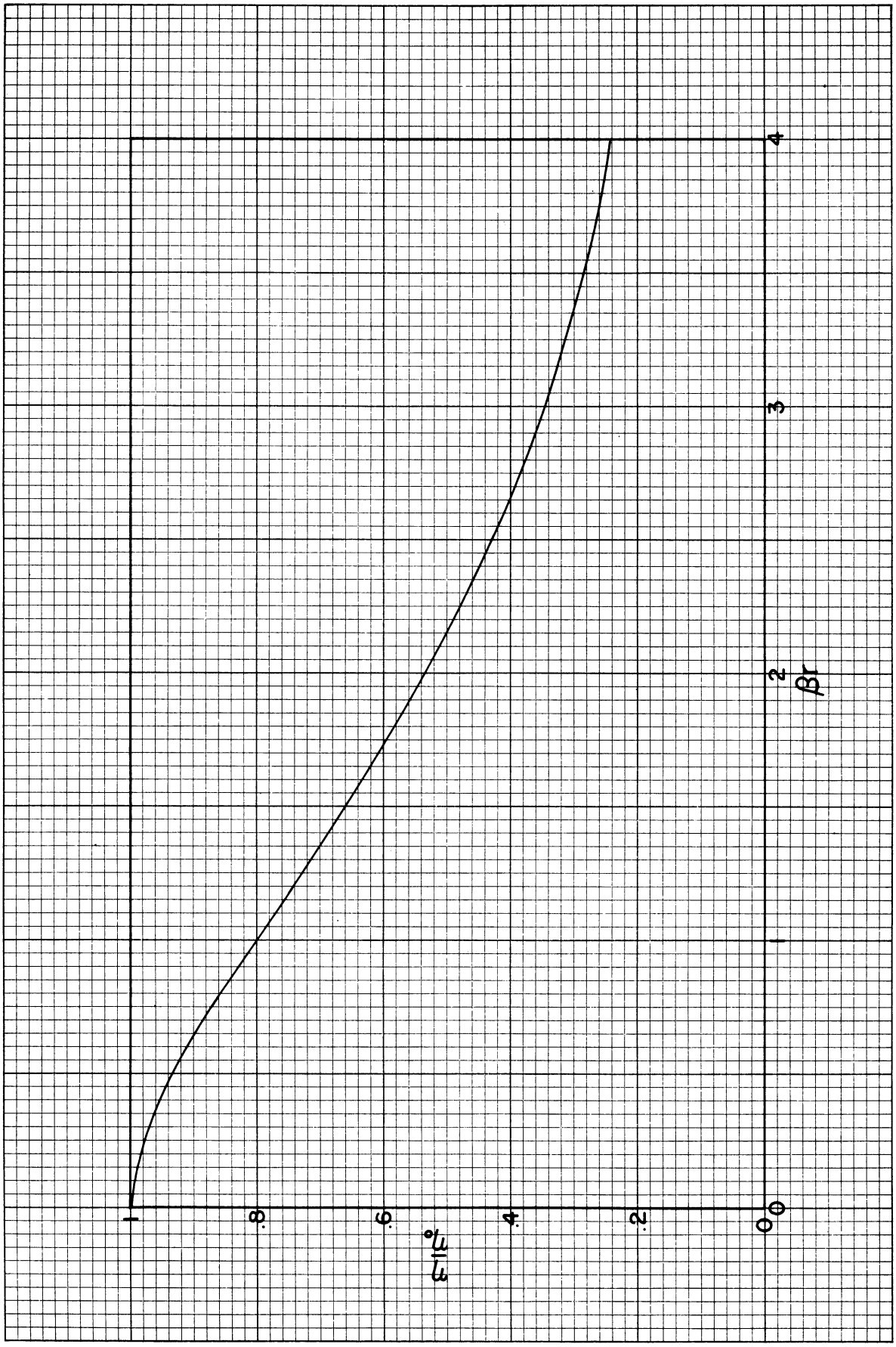

FIG. A-7.--Reduction factor for efficiency.

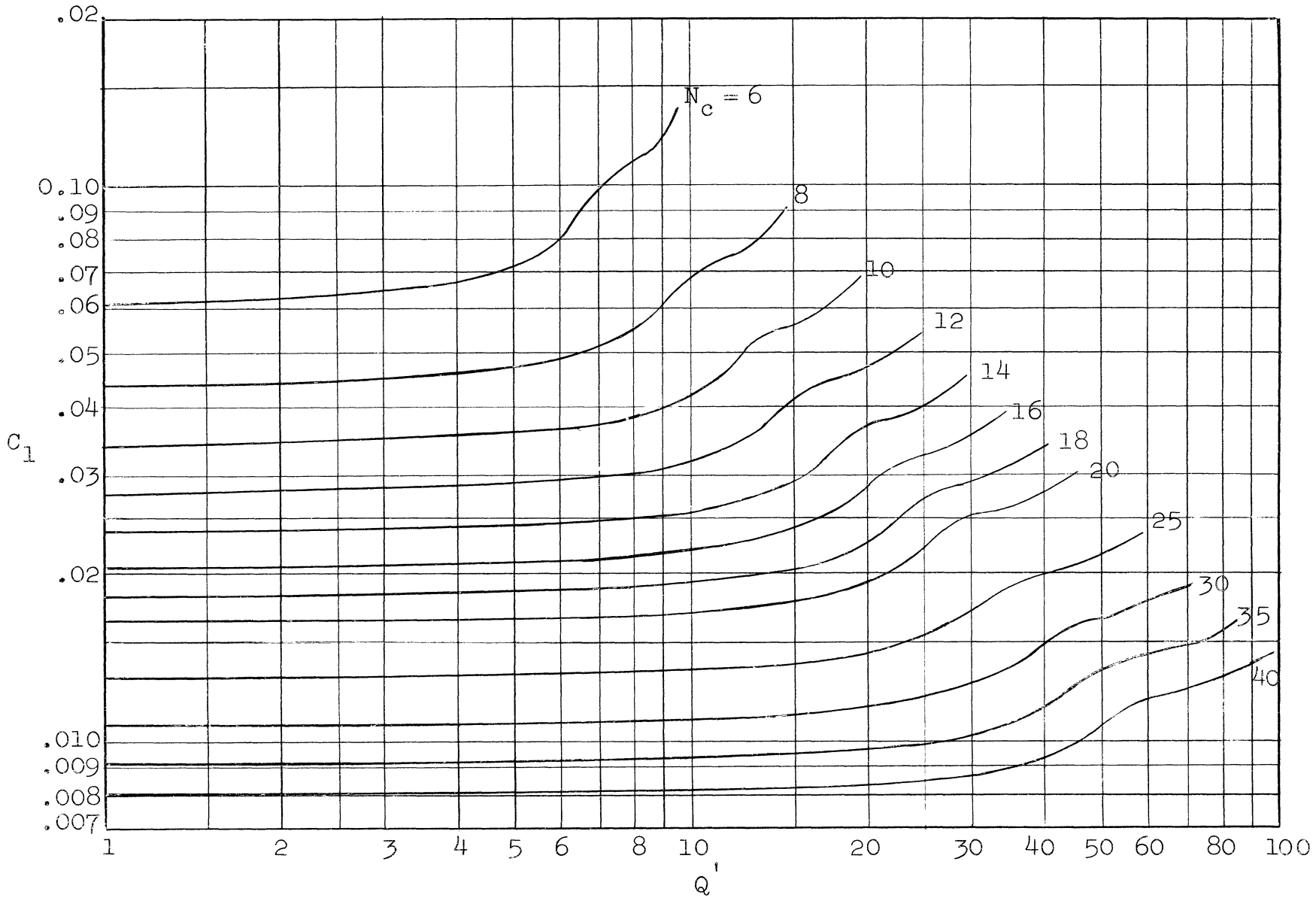

FIG. A-8.--Chart for computing starting currents. $I_{start} = C_1^3/K$, where K is given by Eq. (A-20). Q' and N_c are given by Eqs. (A-19) and (A-22) respectively.

REFERENCES

1. R. W. Grow and D. A. Watkins, "Backward-wave oscillator efficiency," Proc. IRE, vol. 43, July 1955, pp. 848-56.
2. H. Heffner, "Analysis of the backward-wave traveling-wave tube," Proc. IRE, vol. 42, June 1954, pp. 930-37.
3. H. R. Johnson, "Backward-wave oscillators," Proc. IRE, vol. 43, June 1955, pp. 684-97.
4. J. L. Putz, W. R. Luebke, W. A. Harman, and K. R. Spangenberg, "Operating characteristics of a folded-line traveling-wave tube," TR-No. 15 (N6onr 25132), Stanford University (Electronics Research Laboratory), 10 July 1952.
5. J. R. Pierce, Traveling-Wave Tubes, Van Nostrand, New York, 1950.
6. M. H. Steward, "Traveling-wave tubes using slow-wave structures," TR-No. 16 (N6onr 25132), Stanford University (Electronics Research Laboratory), 31 July 1952.
7. W. A. Harman, "Backward-wave interaction in helix-type tubes," TR-No. 13 (Nonr 22510), Stanford University (Electronics Research Laboratory), 26 April 1954.
8. J. R. Pierce, Theory and Design of Electron Beams, Van Nostrand, New York, 1949, pp. 161-64.
9. J. C. Turnbull, "A high-conductivity glass-to-metal seal," RCA Review, vol. XIII, September 1952, pp. 291-299.
10. J. A. Pask, "New techniques in glass-to-metal sealing," Proc. IRE, vol. 36, February 1948, pp. 286-89.

Report Distribution List

For Technical Report No. 182-1

cc	Addressee
	Chief of Naval Research Department of the Navy Washington 25, D.C.
7	Attn: Code 427
1	Commanding Officer Office of Naval Research Branch Office 1000 Geary Street San Francisco, California
1	Commanding Officer Office of Naval Research Branch Office 1030 E. Green Street Pasadena, California
1	Commanding Officer Office of Naval Research Branch Office John Crerar Library Bldg. 86 E. Randolph Street Chicago 1, Illinois
1	Commanding Officer Office of Naval Research Branch Office 346 Broadway Street. New York 13, New York
1	Officer-in-Charge Office of Naval Research Navy 100 Fleet Post Office New York, New York
	Director Naval Research Laboratory Washington 25, D.C.
1	Attn: Code 2000
1	Attn: Code 5430
1	Attn: Code 5330
1	Attn: Code 5200
1	Attn: Code 5300
1	Attn: Code 5400
1	Attn: Code 2021
1	Attn: Code 5430
	Chief, Bureau of Ships Navy Department Washington 25, D.C.
1	Attn: Code 810
1	Attn: Code 816
1	Attn: Code 820
1	Attn: Code 840
	Chief, Bureau of Aeronautics Navy Department Washington 25, D.C.
1	Attn: EL4
2	Attn: EL45
1	Attn: EL43
	Chief, Bureau of Ordnance Navy Department Washington 25, D.C.
1	Attn: Re 4
1	Attn: Re 9
1	Attn: Re 9d
	Chief of Naval Operations Navy Department Washington 25, D.C.
1	Attn: Code Op 30X
1	Attn: Code Op 371C
1	Director Naval Ordnance Laboratory White Oak, Maryland
1	Director Naval Electronics Laboratory San Diego 52, California
1	U.S. Naval Post Graduate School Monterey, California
	Commander Naval Air Missile Test Center Point Mugu, California
1	Attn: Code 366
1	Attn: Code M T 6
1	U.S. Naval Proving Ground Dahlgren, Virginia
1	Commander U.S. Naval Air Development Center Johnsville, Pennsylvania
1	Commanding Officer New York Naval Shipyard Material Laboratory Library Naval Base Brooklyn, New York
	Naval Ordnance Laboratory Corona, California
1	Attn: Ralph A. Lamm, Chief Missile Development Div.
1	Scientific Research Section Research Branch, R-D Division Office of Asst. Chief of Staff, G4 Department of the Army Washington 25, D.C.
	Chief, E & T Division Office of Chief Signal Officer Department of the Army Washington 25, D.C.
1	Attn: SIGGD
1	Attn: SIGGE-C
1	Attn: SIGEB
	Chief, P & O Division Office of Chief Signal Officer Department of the Army Washington 25, D.C.
1	Attn: SIGOT-5
1	Office of Chief of Engineers Department of the Army Washington 25, D.C.
	Office of the Chief of Ordnance Department of the Army Washington 25, D.C.
1	Attn: ORDTU

cc	Addressee
20	Transporation Officer Signal Corps Engineering Labs. Evans Signal Laboratory, Bldg. 42 Belmar, New Jersey Marked: For SCEL Accountable Officer Attn: Countermeasures Division
1	Commanding Officer Eng. Research & Development Lab. Ft. Belvior, Virginia
1	Commanding Officer Frankford Arsenal Bridesburg, Philadelphia Pennsylvania
	Ballistics Research Laboratory Aberdeen Proving Ground, Maryland
1	Attn: D.W.W. Delsasso
1	Commanding Officer Electronic Warfare Center Fort Monmouth, New Jersey
1	Commanding Officer White Sands Signal Corps Agency 9577th TSU White Sands Proving Grounds Las Cruces, New Mexico
1	Attn; SIGWS-CM
	Commander Wright Air Development Center Wright-Patterson Air Force Base Ohio
2	Attn: WCREO-2
4	Attn: WCLGL
1	Attn: WCLGL-7
1	Attn: WCLRA
1	Attn: WCRR
1	Attn: WCRRH
1	Attn: WCLRR-3
	Chief of Staff United States Air Force Washington 25, D.C.
2	Attn: AFDRD-SC-3
	Commanding General Rome Air Development Center Griffiss Air Force Base Rome, New York
2	Attn: RCRW
1	Attn: Electronic Research Laboratory
	Commander Air Force Cambridge Research Center Air Research and Development Command L.G. Hanscom Field, Bedford, Mass.
2	Attn: CRTOTT-2, Electronics
2	Attn: CRTOTT-2
1	Commander Patrick Air Force Base Cocoa, Florida
	Director Air University Library Maxwell Air Force Base, Alabama
1	Attn: CR 4582
	Commanding General Air Research and Development Command Post Office Box 1395 Baltimore 3, Maryland
1	Attn: RDTDNE
1	Attn: SROPP
1	Commanding General 376th Bomb Wing Barksdale Air Force Base Shreveport, Louisiana
	U.S. Coast Guard 1300 E. Street N.W. Washington 25, D.C.
1	Attn: EEE
	Assistant Secretary of Defense (Research and Development) Research and Development Board Department of Defense Washington 25, D.C.
1	Attn: Technical Library
1	Secretary Committee of Electronics Office of Asst. Secretary of Defense Research and Development Department of Defense Washington 25, D.C.
	Advisory Group on Electron Tubes 346 Broadway, 8th Floor East New York 13, New York
1	Attn: William J. McDonald, Chief Technical Reference Section
1	Attn: H. Tulchin
1	Chief, West Coast Office Signal Corps Eng Labs 75 South Grand Avenue, Bldg 6 Pasadena 2, California
	California Institute of Technology Department of Electrical Engineering Pasadena, California
1	Attn: Prof. L.M. Field
	University of Illinois Control Systems Laboratory Urbana, Illinois
1	Attn: Prof. F. Seitz and Prof. R.E. Norberg
1	Attn: Electrical Engineering Dept.
	Johns Hopkins University Radiation Laboratory 1315 St. Paul Street Baltimore 2, Maryland
1	Attn: Dr. D.D. King
	Massachusetts Institute of Technology Cambridge 39, Massachusetts
1	Attn: Lincoln Laboratory

cc	Addressee
	Ohio State University Department of Electrical Engineering Columbus 10, Ohio
1	Attn: Prof. E. M. Boone
	University of Texas Defense Research Laboratory Austin, Texas
1	Attn: Harold D. Krick, Sr.
1	Director Electronics Defense Group Engineering Research Institute University of Michigan Ann Arbor, Michigan
1	Attn: Dr. Welch
1	Electron Tube Laboratory 3506 East Engineering University of Michigan Ann Arbor, Michigan
	University of Michigan Willow Run Research Center Engineering Research Institute Ypsilanti, Michigan
1	Attn: Dr. H. Goode
1	Commanding Officer Signal Corps Electronics Research Unit 9560th TU P.O. Box 205 Mountain View, California
	Airborne Instrument Laboratory 160 Old Country Road Mineola, L.I., New York
1	Attn: Mr. John Dyer
1	Attn: Mr. W.E. Tolles
	Bell Telephone Laboratories Murray Hill Laboratory Murray Hill, New Jersey
1	Attn: Dr. J.R. Pierce
	Federal Telecommunications Labs,Inc. 500 Washington Avenue Nutley, New Jersey
1	Attn: A.K. Wing VIA: Inspector of Naval Material Naval Industrial Res. Shipyard Bldg. 13, Port Newark Newark, New Jersey
	Gilfillan Bros. 1815 Venice Boulevard Los Angeles, California
1	Attn: Countermeasures Laboratory
	Electron Tube Division of the Research Laboratory General Electric Company The Knolls Schenectady, New York
1	Attn: E.D. McArthur
	General Electric Advanced Electronics Center Ithaca, New York
1	Attn: S.M. Kaplan VIA: J.E. Brown, Security Agent
1	Attn: Eleonore R. Buehl, Librarian
	Glenn L. Martin Co. Baltimore, Maryland
1	Attn: Mary E. Ezzo
	Hallicrafters 4401 West 5th Avenue Chicago, Illinois
1	Attn: William Frankart
	Hughes Aircraft Co. Research and Development Library Culver City, California
1	Attn: Mr. John T. Milek
	The Maxson Corporation 460 West 34th Street New York 1, New York
1	Attn: M. Simpson
	Melpar, Inc. 3000 Arlington Blvd. Falls Church, Virginia
1	Attn: Mrs. J. F. Mackenzie
	Motorola, Inc. 4501 Augusta Blvd. Chicago, Illinois
1	Attn: C & E Librarian
1	Hoffman Radio Corporation 3716 South Hill Street Los Angeles 7, California
	The Rand Corporation 1700 Main Street San Monica, California
1	Attn: Margaret Anderson, Librarian
	Raytheon Corporation Waltham, Massachusetts
1	Attn: W. Welsh
1	Attn: Joseph L. Hurff, Government Contracts Division
1	Raytheon Mfg. Co. 148 California Street Newton, Massachusetts
	Sperry Gyroscope Co. Great Neck, L.I., New York
1	Attn: R.L. Wathen
1	Attn: John Lester
1	Attn: Technical Library
	Sylvania Electric Products Inc. 70 Forsyth Street Boston, Massachusetts
1	Attn: Charles E. Arnold
	Sylvania Electric Products, Inc. 500 Evelyn Avenue Mountain View, California
1	Attn: Mr. R.B. Leng, Manager
	Varian Associates 611 Hansen Way Palo Alto, California
1	Attn: Technical Library

cc	Addressee
	Chief, Plans and Operations Division Office of the Chief Signal Officer Department of the Army Washington 25, D.C.
1	Attn: SIGEW-2
	Commanding General Army Electronics Proving Ground Fort Huachuca, Arizona
1	Attn: Dr. Electronics Warfare Dept.
1	Chief, West Coast Office Signal Corps Engineering Lab. 75 South Grand Ave., Bldg. 6 Pasadena 2, California
1	Signal Corps Liaison Office Wright Air Development Ctr, WCOL-9 Post F5, 1st Floor, Bldg. 16 Wright Patterson Air Force, Ohio
	Signal Corps Liaison Office Massachusetts Institute of Technology 77 Massachusetts Avenue, Bldg 20C-116 Cambridge, Massachusetts
1	Attn: A.D. Bedrosian
1	Signal Corps Liaison Officer Ordnance Corps Guided Missile Center Redstone Arsenal, Huntsville, Alabama
1	Commanding Officer U.S. Naval Ordnance Laboratory Silver Springs 19, Maryland
1	Reproducible copy and Armed Services Technical Information Agency, Knott Bldg. 4th and Main Streets, Dayton 2, Ohio
5	Attn: DSC-SA
	Commander Wright Air Development Center Wright Patterson AFB, Ohio
2	Attn: WCLRO-12
2	Attn: WCOSI
1	Attn: WCRTO
	Bureau of Aeronautics Central District Wright-Patterson AFB, Ohio
1	Attn: Electronics Division
	Commander Rome Air Development Center Griffiss Air Force Base, Rome, N.Y.
1	Attn: Research Library, RCRES-4C
	Chief of Staff United States Air Force Washington 25, D.C.
1	Attn: AFDRD EL-2
	Holloman Air Development Center Holloman AFB, Alamogordo, New Mexico
1	Attn: Technical Analysis Division
	Commander Air Proving Ground Command Eglin Air Force Base, Florida
1	Attn: Adj/TRB
	AF Plant Representative Boeing Airplane Company Seattle Air Procurement District Sacramento Air Material Area Seattle 14, Washington
1	Attn: C.L. Hollingsworth, Plant 2
	Air Weapons Research Museum of Science and Industry University of Chicago Chicago 37, Illinois
1	Attn: Col. Paul E. Shanahan
1	General Electric Advanced Electronics Ctr, Cornell University Ithaca, New York
	University of Michigan Willow Run Research Center Ypsilanti, Michigan
1	Attn: Mr. R.L. Ohlsson
1	Standard Rolling Mills 196 Diamond Street Brooklyn, New York
	Dept. of the Air Force Washington 25, D.C.
1	Attn: Col. F.P. Jaques
	Air Technical Intelligence Center Wright-Patterson AFB, Ohio
1	Attn: AFOIN-ATIAE-4
	Ohio State University Research Foundation Columbus, Ohio
1	Attn: Tom Tice
1	Polarad Electronics Corporation 43-20 34th Street Long Island City 1, New York
1	Kollsman Instrument Corporation 80-08 45th Avenue Elmhurst, New York
1	American Electronics Labs., Inc. 641 Arch Street Philadelphia 6, Pennsylvania
1	Radiomarine Corporation of America 75 Varick Street New York 10, New York
1	Haller, Raymond & Brown, Inc. 124 N. Atherton Street State College, Pennsylvania
1	Scientific Specialities Company Snow & Union Street Boston 35, Massachusetts
	Director of Research Division College of Engineering, New York Univ. New York, New York
1	Attn: Mr. R.F. Cotellessee
1	A.R.F. Products, Inc. 7626 W. Lake Street River Forest, Illinois